Air quality improvement in response to intensified control strategies in Beijing during 2013–2019

Wenjun Li[a], Longyi Shao[a,*], Wenhua Wang[a], Hong Li[b], Xinming Wang[c], Yaowei Li[a], Weijun Li[d], Tim Jones[e], Daizhou Zhang[f]

[a] College of Geoscience and Surveying Engineering, China University of Mining and Technology (Beijing), Beijing 100083, China
[b] State Key Laboratory of Environmental Criteria and Risk Assessment, Chinese Research Academy of Environmental Sciences, Beijing 100012, China
[c] State Key Laboratory of Organic Geochemistry and Guangdong Key Laboratory of Environmental Protection and Resources Utilization, Guangzhou Institute of Geochemistry, Chinese Academy of Sciences, Guangzhou 510640, China
[d] Department of Atmospheric Sciences, School of Earth Sciences, Zhejiang University, Hangzhou 310027, China
[e] School of Earth and Ocean Sciences, Cardiff University, Museum Avenue, Cardiff, CF10, 3YE, UK
[f] Faculty of Environmental and Symbiotic Sciences, Prefectural University of Kumamoto, Kumamoto 862-8502, Japan

First Author: Wenjun Li, (1992-), Ph. D candidate. Email: liwenjun_620@126.com
* Corresponding author: Longyi Shao, (1964-). Email: shaol@cumtb.edu.cn. Full postal address: No. 11, Xueyuan Rd., Haidian District, Beijing, P. R. China, 100083.

Highlights：

1. The air quality of Beijing before and after two action plans was assessed.
2. SO_2 decreased the most, followed by CO, $PM_{2.5}$, PM_{10}, and NO_2, while O_3 increased slightly.
3. The control of coal consumption played a dominant role in pollutant reduction.
4. The influences from meteorology, pollutant emissions, and energy structure were evaluated.
5. The control measures have proved to be effective in improving Beijing's air quality.

Abstract

The air pollution in Beijing has become of increasing concern in recent years. The central and municipal governments have issued a series of laws, regulations, and strategies to improve ambient air quality. The "Clean Air Action" and the "Comprehensive Action" implemented during 2013–2017 largely addressed this concern. In this study, we assessed the effectiveness of the two action plans by environmental monitoring data and evaluated the influencing factors including meteorology, pollutant emissions, and energy structure. The spatial distributions of air pollutants were analyzed using the Kriging interpolation method. The Principal Component Analysis-Multiple Nonlinear Regression (PCA-MNLR) model was applied to estimate the effects of meteorological factors. The results have shown that Beijing's air quality had a measurable improvement over 2013–2019. "Good air quality" days had the highest increases, and "hazardous air quality" days had the most decreases. The concentration of SO_2 decreased most, followed by CO, $PM_{2.5}$, PM_{10}, and NO_2 in descending order, but O_3 showed a fluctuant increase. The "Comprehensive Action" was more effective than the "Clean Air Action" in reducing heavy pollution days during the heating period. The meteorological normalized values of the main pollutants were lower than the observation data during 2013–2016. However, the observed values became lower than the normalized values after 2017, which indicated beneficial weather conditions in 2017 and afterwards. The emissions of SO_2 and dust significantly decreased while NOx had a slight decrease, and the energy structure changed with a dramatic decrease in coal consumption and an obvious increase in the use of natural gas and electricity. The significant reduction of coal-fired emissions played a dominant role in improving Beijing's air quality, and vehicle emission control should be further enhanced. The results demonstrated the effectiveness of the two action plans and the experience in Beijing should have potential implications for other areas and nations suffering from severe air pollution.

Keywords: Air quality, Clean Air Action, Comprehensive Action, effectiveness evaluation, PCA-MNLR model, Beijing

1. Introduction

In recent decades, China has achieved rapid industrialization and urbanization. As a result, severe air pollution problems appeared and became a major concern in China, especially in Beijing (Wang et al., 2018b; Zhang, 2019; Li et al., 2019b; Xu and Zhang, 2020). Air pollution has generated great public concern due to its influence on atmospheric visibility, human health, and global climate change (Sheehan et al., 2016; Huang et al., 2018; Wang et al., 2019c; Liu et al., 2020). To alleviate air pollution, the Beijing Municipal Government (BMG) formulated a series of control policies, laws, and regulations that focused most on SO_2 and total suspended particulate (TSP) control since 1998 (Wang et al., 2008; Zhang et al., 2016). However, the severe haze episodes still occurred, especially in the heating seasons (autumn and winter). One of these severe pollution episodes happened in January 2013, when the monthly average concentration of $PM_{2.5}$ reached almost 160 μg/m^3, affecting about 1.3 million km^2 and 800 million people in northern China (Huang et al., 2014; Li et al., 2015).

Since then, the State Council of China issued the "Air Pollution Prevention and Control Action Plan" (shorten to the APPCAP) on September 10, 2013 (The State Council of China, 2013). The APPCAP is the first national strategy targeting $PM_{2.5}$ pollution and air quality improvement in China by setting specific quantitative targets and clear time nodes (Feng et al., 2019). In particular, as a key city, the $PM_{2.5}$ concentration of Beijing should be kept below 60 μg/m^3 by 2017. To fulfill the target, Beijing has made further efforts according to the guidance of the APPCAP. The BMG issued its own "Beijing 2013–2017 Clean Air Action Plan" (the Clean Air Action) in September 2013 (BMG, 2013), which implemented much more stringent control measures than ever before. However, heavy pollution days still occurred frequently in the winter of 2016 (Wang et al., 2018a). To accomplish the five-year target the "Action Plan for Comprehensive Control of Atmospheric Pollution in Autumn and Winter of Beijing-Tianjin-Hebei region in 2017–2018" (the Comprehensive Action) was carried out subsequently in autumn 2017 (MEP, 2017). The control measures on coal-fired emissions were enhanced in the heating seasons (generally from 15th November to 15th

March of the next year). By the end of 2017, the annual mean concentration of $PM_{2.5}$ reduced to 58 μg/m^3 from 89.5 μg/m^3 in 2013, which fully achieved the five-year goal of the Clean Air Action (Beijing Environment Statement, 2017). Thereafter, the State Council issued a three-year plan on defending the blue sky during 2018–2020. The "Action Plan for Comprehensive Control of Atmospheric Pollution in Autumn and Winter of Beijing-Tianjin-Hebei region" was annually released both in Beijing and its surrounding areas. The annual mean concentration of $PM_{2.5}$ has decreased to 51 μg/m^3 in 2018 and 42 μg/m^3 in 2019, indicating that Beijing's air quality has improved yearly (Beijing Ecology and Environment Statement, 2019).

Analysis of the air pollution characteristics of Beijing and its prominent air pollution control approach after the Clean Air Action can provide valuable guidance in optimizing control measures for policymakers. A significant body of research has shown that pollutant emission controls played a dominant role in the decrease of $PM_{2.5}$ and other pollutants (Zhang et al., 2019b), and the meteorological factors, secondary formation, and regional transport from the surrounding area had a significant influence as well (Cai et al., 2017; Cheng et al., 2019a; Zhang, 2019). A large number of studies have evaluated the air quality improvement by air quality data from online monitoring (Liang et al., 2016; Cui et al., 2019; Chang et al., 2019), offline ground observation (Ma et al., 2017; Wang et al., 2019d; Yang et al., 2020), and remote sensing (Wu et al., 2016; Li et al., 2019a; Geng et al., 2019). Chemical transport models, such as CAMx, WRF-Chem, and WRF-CMAQ (Zhang et al., 2019a; Geng et al., 2019; Zhang et al., 2019b), were frequently applied to analyze the intrinsic mechanism and influencing factors. Xue et al. (2019) found the national population-weighted annual mean $PM_{2.5}$ decreased by 32% in China during 2013–2017. Chen et al. (2019) found that the control of anthropogenic emissions contributed to 80% of the decrease in $PM_{2.5}$ concentration in Beijing 2013–2017. Statistical models, such as the deep neural network model, convergent cross-mapping (CCM) method, and the difference-in-difference (DID) model are other methods to decouple the influencing factors such as meteorology, pollutant emissions (Cobourn et al., 2010; Chen et al., 2018b; Wang et al., 2019a). Vu et al. (2019) found the primary emission controls have led to reductions in $PM_{2.5}$, PM_{10},

NO_2, SO_2, and CO of about 34%, 24%, 17%, 68%, and 33% during 2013–2017 in Beijing, after meteorological correction.

Most of these studies were either concentrated on the long-term effect evaluation of certain air pollutants or focused on the short-term for one season or one year period. These studies could provide valuable insights into the effectiveness of the Clean Air Action. However, the simulations usually have biases compared with ground observations because of the uncertainties in the emission inventory and the missing mechanisms in models, as well as the heavy workload and massive volume of multiple data. Indeed, it is hard to measure the effectiveness of a policy due to compound factors and inner mechanisms, and the relationships among multiple air pollutants are non-linear related. Therefore, it is necessary to analyze both the spatio-temporal patterns of air pollutants and the influencing factors.

In this study, we compared the effectiveness of the Clean Air Action and the Comprehensive Action against the environmental monitoring data in Beijing during 2013–2019, and analyzed the influencing factors of meteorology, emission reduction, and energy structure. The spatial distribution of six air pollutants in Beijing during 2013–2019 was analyzed by the Kriging interpolation method for the first time. The PCA-MNLR model was applied to estimate the influences of meteorological factors. In comparison with the previous researches, this is the first attempt to integrate investigation of the spatio-temporal patterns of six types of air pollutants and the quantitative simulation of the influencing factors over Beijing during 2013–2019. We hope Beijing's experience could be beneficial for other megacities in the world suffering from similar air pollution problems.

2. Data and methods

2.1. Study area

As the capital, political and cultural center of China, Beijing (39.13°–41.08° N and 115.22°–117.50° E) is located in the northwest part of the North China Plain, surrounded by the northern Yanshan Mountains and the western Taihang Mountains (Fig. 1). Beijing has a typical temperate and monsoonal climate with high humidity summers and cold, windy, and dry winters. Moreover, Beijing covers a total provincial area of 16,410 km^2 with a population of 21.5 million (BSY, 2019). The central urban areas of Beijing include six districts, i. e. Haidian (HD), Chaoyang (CY), Dongcheng (DC), Xicheng (XC), Fengtai (FT), and Shijingshan (STS).

2.2. Data sources

In this study, air quality data was obtained from the Beijing ambient air automatic monitoring system. This system consists of 35 air monitoring stations, including 12 state-controlled stations and 23 city-controlled stations (Fig. 1). The real-time data are released to the public by the Beijing municipal environmental monitoring center (BMEMC) (http://www.bjmemc.com.cn/). The data was downloaded from the websites (https://github.com/tuanvvu and http://beijingair.sinaapp.com/#messy), where the real-time values are recorded. Data from the 35 monitoring stations included the hourly value of air pollutants from January 17th, 2013 to February 29th, 2020, and air quality index (AQI) from January 1st, 2014 to February 29th, 2020. The air pollutants consisted of $PM_{2.5}$, PM_{10}, SO_2, NO_2, CO, and O_3. These pollutants are measured by the Thermo Fisher instrument series, which are calibrated by standard gases every two days (Wang et al., 2015). The measurement method and instrument for each pollutant are shown in Table S1. On the other hand, AQI is a comprehensive index calculated by considering six major pollutants, which could reflect the overall air quality (Zhan et al., 2018; Tian et al., 2019).

The pollutant emission data included the annual mean concentration of SO_2, NOx, and dust emissions. The socio-economic data included the annual mean of the permanent population, total energy consumption, gross domestic product (GDP), and vehicle numbers. The energy structure data included the annual means of coal, petroleum, natural gas, and electricity consumption (BSY, 2019). Hourly meteorological data including temperature, relative humidity (RH), wind speed (WS), atmospheric pressure (AP), and visibility (VIS) from January 1st, 2013 to February 29th, 2020, and were downloaded from the website (http://hz.zc12369.com/home/).

2.3. Data analysis

We calculated the AQI daily mean values in 2013 by Eq. (1) and Eq. (2) according to the technical regulations on ambient air quality index (HJ633–2012). The individual air quality index (IAQI) is the air quality index of each air pollutant. AQI and IAQI are dimensionless indexes. The corresponding threshold of each pollutant was presented in Table 1.

$$IAQI_p = \frac{IAQI_{Hi} - IAQI_{Lo}}{BP_{Hi} - BP_{Lo}}\left(C_p - BP_{Lo}\right) + IAQI_{Lo} \quad \text{Eq. (1)}$$

$$AQI = \max\{IAQI_1, IAQI_2, IAQI_3, \ldots, IAQI_6\} \quad \text{Eq. (2)}$$

where $IAQI_p$ is the index for pollutant p, C_p is the concentration of pollutant p, BP_{Hi}/BP_{Lo} is the breakpoint that is greater/less than or equal to C_p, $IAQI_{Hi}/IAQI_{Lo}$ is the AQI value corresponding to BP_{Hi}/BP_{Lo}. The maximum of the $IAQI$ is defined by the value of AQI.

Depend on the different extent of human health impacts regulated by Table 2 according to the technical regulations on ambient air quality index (HJ633–2012), AQI is subdivided to different levels of air quality, including the levels of good (AQI: 0–50), moderate (AQI: 51–100), unhealthy for sensitive groups (AQI: 100–150), unhealthy (AQI: 150–200), very unhealthy (AQI: 200–300), and hazardous (AQI: >300).

The daily average, monthly average, seasonal average, and the annual average of air pollutant concentration and AQI were calculated by the arithmetic mean method. The average of 12 state-controlled stations was used to represent the overall air quality of Beijing. The daily average value was obtained by averaging hourly data from 00:00 to 23:00. As some data were missing due to instrument failure or internet error, and some data were considered abnormal, observation for at least 20 hours is required to obtain a daily average concentration of each pollutant for each station. Moreover, at least 27 days and 324 days are required to obtain monthly and annual average concentration, respectively. Otherwise, the invalid data was excluded. All calculations were carried out according to the National Ambient Air Quality Standards (GB3095–2012) (Table 3), technical regulations on ambient air quality index (HJ633–2012) (http://www.gov.cn/zwgk/2012-03/02/content_2081374.htm), and technical regulations for ambient air quality assessment (HJ663–2013) (http://www.mee.gov.cn/ywgz/fgbz/bz/bzwb/jcffbz/201309/t20130925_260809.shtml).

The concentrations of air pollutants have strong spatial self-aggregation effects, which proved the necessity for regional integration of air quality management (Chen et al., 2019b). For Beijing, the geographical location, land use, and types of the functional zones for monitoring stations are different. To obtain spatial variations of air pollutants in Beijing, we employed geographic information system (GIS) which could facilitate the understanding at spatial perspectives, and conducted the Kriging interpolation method which is a typical statistical algorithm widely applied in geoscience and atmospheric science (Liu et al., 2017; Hu et al., 2019). We applied the Kriging method using ArcGIS 10.2 software to investigate the spatial distribution of air pollutants from 35 monitoring stations in Beijing.

2.4. PCA-MNLR method

In this study, a multiple nonlinear regression (MNLR) method was employed to analyze the relationship between meteorological variables; namely temperature, relative humidity (RH), wind speed (WS), atmospheric pressure (AP), and visibility (VIS), and six air pollutant concentrations variables; namely $PM_{2.5}$, PM_{10}, SO_2, NO_2, CO, and O_3. The regression model requires a low correlation between variables, otherwise, the multicollinearity will affect the accuracy of the simulation results. Thus, the Principal Component Analysis (PCA) method was used to find patterns in data of high dimension by reducing the dimensionality (Salim et al., 2019; Li et al., 2018). As a simple, quick, and accurate statistical method, the Principal Component Analysis-Multiple Nonlinear Regression (PCA-MNLR) method, or named principal components regression (PCR), was employed by using the MATLAB R2019b software (MathWorks, Natick, MA, USA). PCA-MNLR method has been applied for predicting air pollution by several studies (Tan et al., 2016; Li et al., 2018).

The meteorological factors were set as independent variables, and the air pollutant concentrations were set as dependent variables. Firstly, the described data dependency by Eq. (3) found strong correlations in most of the dependent variables. Due to the complex natural environment, there are different dimensions between environmental data, such as $PM_{2.5}$ (μg/m^3) and temperature (℃). Data were firstly nondimensionalized into proper dimensionless indexes by the Eq. (4).

$$R(X,Y) = \frac{\sum_{i=0}^{n}(x_i-\overline{x})(y_i-\overline{y})}{\sqrt{\sum_{i=0}^{n}(x_i-\overline{x})^2}\sqrt{\sum_{i=0}^{n}(y_i-\overline{y})^2}} \quad \text{Eq. (3)}$$

$$z_{ij} = \frac{x_{ij}-\min(x_{ij})}{\max(x_{ij})-\min(x_{ij})} \quad \text{Eq. (4)}$$

In Eq. (3), where *R(X, Y)* represents the correlation coefficient between two dependent variables. The closer of $|R(X,Y)|$ to 1, the more correlative between *X* and *Y*, and the nearer to 0, the more unobvious correlative between *X* and *Y*. In Eq. (4), where *i* is the year, *j* is the number index, x_{ij} is the data of *j* index in *i* year, $min(x_{ij})$ is the minimum value of *j*th index, and $max(x_{ij})$ is the maximum value of *j*th index.

The above data was principal component transformed to get the eigenvector matrix Coeff, the score matrix Score (Y), and the eigenvalue matrix latent. After the PCA process, the correlations in dependent variables were checked again. Due to the nonlinear relationship between the influencing factors, a power function was employed to perform the multivariate non-linear regression analysis by Eq. (5), and the natural logarithm of both sides of Eq. (5) were taken by Eq. (6).

$$y = \alpha_0 X_1^{a_1} X_2^{a_2} \cdots X_k^{a_k} \quad \text{Eq. (5)}$$

$$\ln(y) = a_0 + a_1 lnX_1 + a_2 lnX_2 + \cdots + a_k lnX_k \quad \text{Eq. (6)}$$

2.5. Control measures

Based on nearly 20 years of air pollution control, China has issued a series of strong air pollution prevention and control programs and ultimately developed a rich experience in air quality management (UN Environment, 2019). In the APPCAP, as a milestone, the control pollutants changed from the traditional pollutants (SO_2, NOx, smoke, and dust) to multiple pollutants including SO_2, NOx, primary particulate matter, and volatile organic compounds (VOCs). Non-point source pollution controls had been greatly strengthened instead of the previous industrial point sources. The key control regions included the Beijing-Tianjin-Hebei (BTH) area, the Yangtze River Delta (YRD), and the Pearl River Delta (PRD). The APPCAP is for nationwide control while the Clean Air Action is set by Beijing for the local emissions control. Particularly, as the principal action plans for Beijing, the Clean Air Action emphasized the integrated control measures, and the Comprehensive Action focused on the coal-fired emission reductions in autumn and winter that played a dominant role in its air quality improvement during 2013–2019. These measures greatly reduced coal-fired emissions. The major control measures of these two action plans are given in Table 4.

3. Results

3.1. Trends of AQI

During 2013–2019, the overall air quality in Beijing has improved dramatically, with the annual mean AQI decreasing year by year (Fig. 2). The proportion of meeting-standard days (AQI < 100) increased from 48.4% to 66.8%, and heavy pollution days (AQI > 200) decreased from 15.4% to 1.1%. During these seven years, the number of good air quality days had the most significant increase (111.7%), followed by moderate air quality days (16.9%) and unhealthy for sensitive (5.8%) in descending order. In association with these increases, hazardous days had the greatest decrease, falling from 14 days to zero, followed by very unhealthy days (90.6%) and the unhealthy days (40.7%).

Fig. 3 shows the time-series of the daily average of AQI. In northern China, heavy pollution days mostly happen in autumn and winter due to the central heating (Qiu et al., 2017). After the Clean Air Action implemented in 2013, the heavy air pollution days decreased in spring (4.1%), summer (70%), and autumn (6.6%) during 2013–2016, while the heavy air pollution days increased by 44.8% in winter. After the stringent control measures of the Comprehensive Plan implemented in autumn 2017, the daily value of AQI had a dramatic decrease (shown by the red circles in Fig. 3). During 2016–2017, heavy pollution days dramatically decreased by 88% in winter and 78.6% in autumn, and the meeting-standard days increased by 57.0% in winter and 32.4% in autumn. Therefore, compared to the Clean Air Action, the Comprehensive Action is more effective in reducing the heavy pollution days in the heating seasons.

3.2. Trends of air pollutants

Between 2013 and 2019, the annual mean concentration of $PM_{2.5}$, PM_{10}, SO_2, NO_2, and CO decreased by 53.1%, 37.1%, 84.9%, 33.9%, and 58.8%, respectively, while O_3 slightly increased by 4.1% in Beijing (Table 5). During the past seven years, SO_2 had the greatest decrease, followed by CO, $PM_{2.5}$, PM_{10}, and NO_2 in descending order. However, O_3 increased in 2013–2015 and then decreased after 2016; the annual average of O_3 in 2019 was still higher than in 2013. Compared to the National Ambient Air Quality Standard II, the annual mean concentrations of SO_2 and CO in 2019 were much lower than the standard, and NO_2 and PM_{10} were 7.5% and 2.9% lower than the standard, which was the first time the standard was reached in recent years. However, $PM_{2.5}$ and O_3 were still 20.0% and 19.4% higher than the standard, respectively. In conclusion, under the implementation of the Clean Air Action and the Comprehensive Action from 2013 to 2019, the reductions of SO_2 and CO were very significant, but a complicated type of compound $PM_{2.5}$ and O_3 pollution emerged (Jin et al., 2016).

Fig. 4 shows the trends in the daily average, monthly average, and seasonal average of air pollutants. The concentrations of $PM_{2.5}$ were higher in autumn and winter than in spring and summer. The seasonal distributions of PM_{10}, SO_2, NO_2, and CO were approximately similar to $PM_{2.5}$. Typically, air pollution is worse in autumn and winter, while air quality is relatively better in summer over this region (Zhang et al., 2018). Thus, the seasonal characteristics of $PM_{2.5}$, PM_{10}, SO_2, NO_2, and CO showed a single valley distribution with the minimum appeared in summer. However, O_3 had a different seasonal variation compared to other pollutants, with higher concentrations in summer and spring, and lower concentrations in autumn and winter, which often showed as a single peak distribution with the maximum appeared in summer. The concentration of SO_2 and CO decreased significantly in autumn and winter, which were close to the values in spring and summer, so the trend in the seasonal distributions of SO_2 and CO tended to be flat. However, the trends in $PM_{2.5}$, PM_{10}, NO_2, and O_3 still fluctuated throughout the whole year.

3.3. Temporal and spatial distribution of air pollutants in heating and non-heating periods

Before the Clean Air Action, the heat supply in Beijing was mainly by coal-fired boilers, and the coal consumption was usually higher in the heating period, which could directly aggravate haze pollution. After the implementation of the Clean Air Action, the clean energy alternatives such as coal-to-gas or coal-to-electricity gradually took over the coal-fired boilers in the heating seasons (Xu and Ge, 2020). To compare the coal consumption in the heating seasons of these two action plans, the research period was divided into two stages, including stage I (between the Clean Air Action and the Comprehensive Action) and stage II (after the Comprehensive Action).

At stage I, the concentrations of $PM_{2.5}$, PM_{10}, SO_2, CO, and NO_2 in the heating period remained much higher than in the non-heating period, while these concentrations significantly declined at stage II (Fig. 5). Compared to 2016, $PM_{2.5}$, PM_{10}, SO_2, CO, and NO_2 in the heating period of 2017 had decreased by 48.5%, 39.4%, 47.7%, 46.3%, and 29.7%, respectively (Fig. S1). Especially in 2017, $PM_{2.5}$ and PM_{10} in the heating period were 10.3% and 17.0% lower than in the non-heating period (Fig. S1). These decreases were substantially related to the changing levels of coal consumption in the heating seasons after the implementation of the Comprehensive Action. Decreasing emissions from the coal-burning section are the key factor to control pollution during the heating season (Qiu et al., 2017). Unlike other pollutants, the concentrations of O_3 were much higher in the non-heating period. At stage II, O_3 even increased in both the heating period and the non-heating period. In summary, haze pollutions dominated by particulate matter were controlled effectively, especially in the heating seasons, but photochemical pollutions dominated by O_3 became increasingly prominent.

The vehicle emissions are always higher in the central urban areas with high traffic density, and have no seasonal variations, while the coal-fired emissions tend to display a seasonal variation with higher concentrations in the heating period. As Fig. 6 shows, the spatial distributions of coal-fired pollutants including $PM_{2.5}$, PM_{10}, SO_2, and CO were similar. These pollutants had higher concentrations in the southern and central urban areas and relatively lower concentrations in the northern regions, which is related with the regional transportation from the southern areas of Beijing (Zheng et al., 2015; Zhang et al., 2017). However, NO_2 and O_3 had different distribution patterns. The serious NO_2 pollution in the heating period was related to the extra coal-fired emission source from heat supply, while in the non-heating period the source of NO_2 mostly came from vehicle emissions. At stage I, the concentrations of NO_2 were high in central urban areas in the non-heating period, and then the high NO_2 regions became wider in the heating period, with a distribution in the southern and central urban areas, which are mainly due to the extra coal consumption for central heating. At stage II, the high NO_2 regions were still centered in the central urban areas with high traffic density, but became much more constrained than stage I. This change was particularly obvious in the heating period. Therefore, the decrease in NO_2 was mainly due to the reduction of NOx from coal-fired emissions in the heating seasons.

Unlike other pollutants, the concentrations of O_3 in the non-heating period were higher than in the heating period. After the strict implementation of the Comprehensive Plan, the concentrations of O_3 increased further, especially in central urban areas during the non-heating period of stage II. In the lower atmosphere, O_3 is a secondary pollutant formed by the photochemical reaction of its precursors including organics like methane, volatile organic compounds (VOCs), and non-methane volatile organic compounds (NMVOCs), CO, and NOx. (Tao et al., 2016). To only focus on NOx emission reduction may not work or even aggravate O_3 pollution, VOCs-targeted control is a more practical and feasible way (Wang et al., 2019b). However, the control of VOCs is difficult due to its non-organizational emissions, and the relationships between O_3 and its precursors are non-linear, making the control of O_3 more challenging. In addition, the concentrations of O_3 were higher in the suburb areas than in the traffic-related central urban areas. Affected by vehicle emissions, the high concentrations of NO and NO_2 promote the reaction of O_3 with NO ($O_3 + NO \rightarrow NO_2 + O_2$) that frequently happens in the urban area in summer, which consumes ozone (Wang et al., 2014). There is also the terrestrial vegetation cover that is also regarded as an important source of VOCs, which could promote O_3 formation in the suburb areas and affect the distribution of O_3 (Maji et al., 2019).

4. Discussion

4.1. Impact of meteorological conditions on air pollutants

The concentrations of air pollutants are closely related to meteorological conditions (Nguyen et al, 2019; Zhang et al., 2019c; Chen et al., 2018a). An important aspect in assessing air quality improvement is to consider the impact of meteorology (Chen et al., 2017; Vu et al., 2019). Beneficial weather conditions with stronger wind speed, higher local mixing layer heights (MLHs) could favour the dispersion of pollutants, while adverse weather conditions with higher relative humidity, lower wind speed, less rainfall, and more inversions, could aggravate air pollution conditions (Xu et al., 2020).

The meteorological factors were estimated by the PCA-MNLR model. Fig. 7 shows the time-series variation of the meteorological normalized concentrations and the observed concentrations of air pollutants during 2013–2019 in Beijing. By comparing the results of observation and simulation, it indicated that the PCA-MNLR model could reproduce the temporal distribution of air pollutants relatively well (R^2: 0.73–0.82). The meteorological normalized values (red line) had regular variations, which were similar to the observation results (black line). During 2013–2016, the meteorological normalized values of SO_2 and CO were just lower than the observed values, which indicated that the real meteorological condition was more significant and this could aggravate the SO_2 and CO pollution. However, after the implementation of the Comprehensive Plan, the meteorological normalized values of SO_2 were higher than the observed values, and the simulation and observation values of CO were close. This was mainly due to the more beneficial weather condition favoring the dispersion of air pollutants. Furthermore, SO_2 and CO had the most significant decreases over the seven years. Previous studies have indicated that, compared with 2013, the meteorological conditions worsened in 2014 and 2015 and improved in 2016 and 2017 (Zhang et al., 2019c). Thus, the beneficial weather conditions in 2017 and afterwards helped the dispersion of pollutants and promoted air quality improvement.

However, this variation pattern was not so consistent with $PM_{2.5}$ and PM_{10}. The differences between the stimulation and observation values of the particles were not so similar as the variation of meteorology. The influencing factors in the concentration of $PM_{2.5}$ and PM_{10} are more complicated, and only considering the relationship between several meteorological conditions and air pollutants is insufficient. Moreover, the meteorological normalized O_3 and NO_2 concentrations were always lower than the observation results, which were different compared to other pollutants. One of the reasons is that the influence of the meteorological factor was different for O_3 and NOx, and the interactions between O_3/NOx and other air pollutants were more complicated. The different meteorological conditions could not completely explain the difference between the observation and simulation values, as previous analyses had indicated that the meteorology contributed about 12.1%–31% of the total $PM_{2.5}$ reduction in Beijing (Zhang et al., 2019c; Cheng et al., 2019a; Cheng et al., 2019b). Although the meteorological conditions significantly influenced the concentration of air pollutants, the dominant factor driving this decrease was still the emission reductions made by strict control measures (Chen et al., 2019a).

In addition, we compared the annual mean concentrations of air pollutants after the meteorological normalization by this study and other references in Table S2. Moreover, the PCA-MNLR results and other WRF-CMAQ modeling results by Cheng et al. (2019a) were compared by the monthly concentrations (Fig. 8). The correlation coefficients between monthly values by PCA-MNLR model was 0.84, while it was 0.78 for the WRF-CMAQ study. The difference between the monthly observation and the simulation values of $PM_{2.5}$ ranged from 0.3% to 23% with an average 10.3% difference by PCA-MNLR. In contrast, the deviation changed to 3%–33.6% with an average of 10.3% for the WRF-CMAQ study.

Fig. 9 shows the score plot of the two principal components. The score plot could help to elucidate the distribution of the observations and reveal the relative relationship between data points. Theoretically, on the score plot, closer distribution means similar behavior between samples (Camacho, 2014). In Fig. 9, each point represented the score status of each day considering both the meteorological factors and air pollutant concentrations. During 2013–2016, the daily meteorological normalized values of some days in autumn and winter were still high (the high x-axis value in Fig. 9), which represented heavy pollution days especially happened in winter. The x-axis values of scores significantly decreased year by year. Especially after 2017, the number of high values points gradually decreased with a reduction in x-axis value. The data points in 2019 were already close to the y-axis with low x-axis values, indicating the significant decrease of heavy pollution days in the whole year and the improvement of air quality in Beijing.

4.2. Impact of emission reduction on air pollutants

The emission reductions in response to intensified control measures greatly affect the ambient air concentrations (Chen et al., 2019a; Cheng et al., 2019b). Fig. 10 shows the variations of SO_2, NOx, and dust emissions during 2010–2018 in Beijing. The primary emissions of SO_2 and dust decreased especially after 2017, while NOx emission was still high although the range decreased. With these decreases, the concentrations of SO_2 decreased most, $PM_{2.5}$ and PM_{10} decreased significantly, especially after the implementation of the Comprehensive Action, while the decreasing range of NO_2 was much less than that of SO_2. SO_2 is mainly emitted from the coal-fired source, while NO_2 from both coal-fired and vehicle sources (Meng et al., 2018). The coal-fired emission control measures were in line with the emission reduction of SO_2 but they were not with NO_2. One of the reasons is that NOx sourced from vehicle emissions were not effectively controlled, mainly due to the less effective control measures on vehicle emissions, such as traffic restrictions (Wang et al., 2019d; Sun et al., 2018; Fontes et al., 2018; Zhang et al., 2020). Meanwhile, the reductions of $PM_{2.5}$ and PM_{10} were mainly due to the result of coal-fired control measures (Cheng et al., 2019a). Moreover, the decrease of PM_{10} was less than $PM_{2.5}$, which was mainly due to the natural sources including the spring dust storms from the desert areas in north and northwest of China (Liu et al., 2014; Li et al., 2017).

4.3. Impact of energy structure variation on air pollutants

The energy support of China mainly relies on fossil fuels, including coal, petroleum, and natural gas. The previous energy structure was dominated by coal, which was mainly due to the small volume and difficult utilization of other energy types, and the costly development of renewable energy (Ji et al., 2019). With continuous air pollution control strategies, the energy consumption structure of Beijing was optimized, with coal consumption decreased 86.8% and natural gas increased 87.9% during 2013–2018 (Fig. 11a). Meanwhile, the socio-economic development had a stable growth with a significant increase in the vehicle population, GDP, total energy consumption, and a notable decrease in major air pollutant concentrations (Fig. 11b). Such an optimized energy structure played an important role in the air quality improvement in Beijing especially by the decrease of coal-fired consumption.

4.4. A comparison of air quality in Beijing with other megacities

Beijing's air quality has been gradually improved in recent years, but the current air pollution levels are still severe. Fig. 12 shows the comparison of $PM_{2.5}$ concentration in Beijing with Shanghai, Shenzhen, and other capital cities around the world. The annual average concentration of $PM_{2.5}$ in Beijing is still much higher than in other capital cities of developed countries, such as Washington DC, London, and Wellington, and other Asian cities, such as Tokyo and Seoul. Meanwhile, the $PM_{2.5}$ concentration of Beijing is also higher than in Chinese domestic cities, such as Shanghai and Shenzhen. However, the $PM_{2.5}$ concentration in Beijing is lower than some cities in developing countries, such as Delhi and Kabul. According to the national standard limit for $PM_{2.5}$, the moderate air quality level set at 75 $\mu g/m^3$ might be relatively high, only being close to the initial transition standard of the WHO. Many studies have proved that the concentration of $PM_{2.5}$ at 35–75 $\mu g/m^3$ could still be harmful to the human body (Di et al., 2017). As the stricter environmental regulations have led to low levels of pollution (Wang et al., 2019a), the air quality standard should be upgraded to maintain a better air quality with a safer $PM_{2.5}$ level. Hence, the control of $PM_{2.5}$ should be intensified depending on a stricter standard. Although O_3 has recently become one of the primary pollutants in Beijing (Beijing Ecology and Environment Statement, 2019), the concentration limit of O_3 is almost in accordance with the international standards (Table 3). Thus, O_3 keeps a low over-standard level when compared to $PM_{2.5}$. Therefore, we should continue to control $PM_{2.5}$ pollution by cutting coal consumption, and strengthen motor vehicle control to mitigate NO_2 and O_3 pollution. The combined control of $PM_{2.5}$ and O_3 is the key for future air pollution control (Xiang et al., 2020).

5. Conclusions

In this study, the air quality improvement under the Clean Air Action and the Comprehensive Action were assessed by the air monitoring data, and the influencing factors including meteorology, pollutant emissions, and energy structure were discussed.

(1) The air quality of Beijing had obvious improvements during 2013–2019, with the most increases in good air quality days and the most decreases in hazardous air quality days. The concentration of SO_2 decreased most, followed by CO, $PM_{2.5}$, PM_{10}, and NO_2 in descending order, except O_3 showed a variable increase.

(2) The Comprehensive Action has been more effective in reducing heavy pollution days in winter, and largely reduced the concentrations of coal-fired air pollutants in heating seasons. In 2017, $PM_{2.5}$ and PM_{10} in the heating period were even lower than those in the non-heating period.

(3) $PM_{2.5}$, PM_{10}, SO_2, and CO concentrations were higher in the southern and central urban areas. The high NO_2 regions became more constrained after the Comprehensive Action, mainly due to the reduction of NOx from coal-fired emissions. However, the O_3 concentrations were higher in the suburb areas than those in the central urban areas.

(4) The meteorological normalized values of SO_2 and CO were lower than the observation data during 2013–2016, and after 2017 these values became higher, which indicated beneficial weather conditions in 2017 and afterwards. But the variation pattern was not as consistent with the changes of $PM_{2.5}$, PM_{10}, NO_2, and O_3, which indicated that the meteorology could not completely explain the difference between the observation and simulation. The decrease of SO_2 and dust emissions achieved a significant decrease in SO_2, $PM_{2.5}$, and PM_{10}, while NOx only had a slight decrease to

get a less decrease in NO_2. The significant reduction of coal-burning played a dominant role in improving Beijing's air quality.

(5) Beijing's air quality management experiences could guide other developing countries in coping with similar air pollution problems.

Acknowledge

This study is supported by the National Natural Science Foundation of China (Grant No. 41175109) and its project for International Cooperation and Exchanges (Grant No. 41571130031), the National Basic Research Program of China (Grant No. 2013CB228503), Beijing Municipal Science & Technology Commission (No. Z181100005418015), and the Yueqi Scholar funds of China University of Mining and Technology (Beijing). All authors declare that they have no competing financial interests.

References

Beijing Ecology and Environment Statement, 2019. Beijing Municipal Ecology and Environment Bureau.http://sthjj.beijing.gov.cn/bjhrb/index/xxgk69/sthjlyzwg/1718880/1718881/1718882/1791057/index.html (accessed 27 April 2020).

Beijing Environment Statement, 2017. Beijing Municipal Ecology and Environment Bureau. http://sthjj.beijing.gov.cn/bjhrb/resource/cms/2018/05/2018051614522475279.pdf (accessed 16 May 2018).

BMG (Beijing Municipal Government), 2013. Beijing 2013–2017 Clean Air Action Plan. http://www.beijing.gov.cn/zhengce/zfwj/zfwj/szfwj/201905/t20190523_72673.html (accessed 12 September 2013).

BSY (Beijing Statistical Yearbooks), 2019. Beijing Municipal Bureau Statistics. http://tjj.beijing.gov.cn/tjsj_31433/.

Cai, S., Wang, Y., Zhao, B., Wang, S., Chang, X., Hao, J., 2017. The impact of the “Air Pollution Prevention and Control Action Plan” on $PM_{2.5}$ concentrations in Jing-Jin-Ji region during 2012–2020. Science of The Total Environment. 580, 197–209. https://doi.org/10.1016/j.scitotenv.2016.11.188.

Camacho, J., 2014. Visualizing Big data with Compressed Score Plots: Approach and research challenges. Chemometrics and Intelligent Laboratory Systems.135: 110–25. https://doi.org/10.1016/j.chemolab.2014.04.011.

Chang, L., Shao, L., Yang, S., Li, J., Zhang, M., Feng, X., Li, Y., 2019. Study on variation characteristics of $PM_{2.5}$ mass concentrations in Beijing after the action on comprehensive control of air pollution. Journal of Mining Science and Technology. 4(6):539–546. 10. 19606 / j. cnki. jmst. 2019. 06. 009.

Chen, L., Guo, B., Huang, J., He, J., Wang, H., Zhang, S., Chen, S.X., 2018a. Assessing air-quality in Beijing-Tianjin-Hebei region: The method and mixed tales of $PM_{2.5}$ and O_3. Atmospheric

Environment. 193, 290–301. 10.1016/j.atmosenv.2018.08.047.

Chen, Z., Xie, X., Cai, J., Chen, D., Gao, B., He, B., Cheng, N., Xu, B., 2018b. Understanding meteorological influences on $PM_{2.5}$ concentrations across China: a temporal and spatial perspective. Atmospheric chemistry and physics. 18, 5343–58. https://doi.org/10.5194/acp-18-5343-2018.

Chen, Z., Cai, J., Gao, B., Xu, B., Dai, S., He, B., Xie, X., 2017. Detecting the causality influence of individual meteorological factors on local $PM_{2.5}$ concentration in the Jing-Jin-Ji region. Scientific Reports. 7(1): 40735. 10.1038/srep40735.

Chen, Z., Chen, D., Kwan, M., Chen, B., Gao, B., Zhuang, Y., Li, R., Xu, B., 2019a. The control of anthropogenic emissions contributed to 80% of the decrease in $PM_{2.5}$ concentrations in Beijing from 2013 to 2017. Atmospheric Chemistry and Physics. 19(21), 13519–13533. https://doi.org/10.5194/acp-19-13519-2019.

Chen, Z., Chen, D., Xie, X., Cai, J., Zhuang, Y., Cheng, N., He, B., Gao, B., 2019b. Spatial self-aggregation effects and national division of city-level $PM_{2.5}$ concentrations in China based on spatio-temporal clustering. Journal of Cleaner Production. 207:875–81. 10.1016/j.jclepro.2018.10.080.

Cheng, J., Su, J., Cui, T., Li, X., Dong, X., Sun, F., Yang, Y., Tong, D., Zheng, Y., Li, Y., Li, J., Zhang, Q., He, H., 2019a. Dominant role of emission reduction in $PM_{2.5}$ air quality improvement in Beijing during 2013–2017: a model-based decomposition analysis. Atmospheric Chemistry and Physics. 19, 6125–6146. https://doi.org/10.5194/acp-19-6125-2019.

Cheng, N., Cheng, B., Li, S., Ning, T., 2019b. Effects of meteorology and emission reduction measures on air pollution in Beijing during heating seasons. Atmospheric Pollution Research. 10(3): 971–9. https://doi.org/10.1016/j.apr.2019.01.005.

Cobourn, W.G., 2010. An enhanced $PM_{2.5}$ air quality forecast model based on nonlinear regression and back-trajectory concentrations. Atmospheric Environment. 44, 3015–3023. https://doi.org/10.1016/j.atmosenv.2010.05.009.

Cui, J., Lang, J., Chen, T., Mao, S., Cheng, S., Wang, Z., Cheng, N., 2019. A framework for investigating the air quality variation characteristics based on the monitoring data: Case study for Beijing during 2013–2016. Journal of Environmental Sciences. 81, 225–237. https://doi.org/10.1016/j.jes.2019.01.009.

Di, Q., Wang, Y., Zanobetti, A., Wang, Y., Koutrakis, P., Choirat, C., Dominici, F., Schwartz, J.D., 2017. Air Pollution and Mortality in the Medicare Population. N Engl J Med. 376, 2513–2522. 10.1056/NEJMoa1702747.

Feng, Y., Ning, M., Lei, Y., Sun, Y., Liu, W., Wang, J., 2019. Defending blue sky in China: Effectiveness of the "Air Pollution Prevention and Control Action Plan" on air quality improvements from 2013 to 2017. Journal of Environmental Management. 252:109603. https://doi.org/10.1016/j.jenvman.2019.109603.

Fontes, T., Li, P., Barros, N., Zhao, P., 2018. A proposed methodology for impact assessment of air quality traffic-related measures: The case of $PM_{2.5}$ in Beijing. Environmental Pollution. 239, 818–828. https://doi.org/10.1016/j.envpol.2018.04.061.

Geng, G., Xiao, Q., Zheng, Y., Tong, D., Zhang, Y., Zhang, X., Zhang, Q., He, H., Liu, Y., 2019. Impact of China's Air Pollution Prevention and Control Action Plan on $PM_{2.5}$ chemical composition over eastern China. Science China (Earth Sciences). 62(12): 1872–84. https://doi.org/10.1007/s11430-018-9353-x.

Hu, H., Hu, Z., Zhong, K., Xu, J., Zhang, F., Zhao, Y., Wu, P., 2019. Satellite-based high-resolution mapping of ground-level $PM_{2.5}$ concentrations over East China using a spatiotemporal regression kriging model. Science of The Total Environment. 672: 479–90. https://doi.org/10.1016/j.scitotenv.2019.03.480.

Huang, J., Pan, X., Guo, X., Li, G., 2018. Health impact of China's Air Pollution Prevention and Control Action Plan: an analysis of national air quality monitoring and mortality data. The Lancet Planetary Health. 2(7), e313–e323. https://doi.org/10.1016/S2542-5196(18)30141-4.

Huang, R.-J., Zhang, Y., Bozzetti, C., Ho, K.-F., Cao, J.-J., Han, Y., Daellenbach, K.R., Slowik, J.G., Platt, S.M., Canonaco, F., Zotter, P., Wolf, R., Pieber, S.M., Bruns, E.A., Crippa, M., Ciarelli, G., Piazzalunga, A., Schwikowski, M., Abbaszade, G., Schnelle-Kreis, J., Zimmermann, R., An, Z., Szidat, S., Baltensperger, U., Haddad, I.E., Prévôt, A.S.H., 2014. High secondary aerosol contribution to particulate pollution during haze events in China. Nature. 514, 218–222. https://doi.org/10.1038/nature13774.

Ji, Q., Zhang, D.. 2019. How much does financial development contribute to renewable energy growth and upgrading of energy structure in China? Energy Policy. 128, 114–124. https://doi.org/10.1016/j.enpol.2018.12.047.

Jin, Y., Andersson, H., Zhang, S., 2016. Air pollution control policies in China: a retrospective and prospects. International Journal of Environmental Research and Public Health. 13 (12), 1219. https://doi.org/10.3390/ijerph13121219.

Li, D., Liu, J., Zhang, J., Gui, H., Du, P., Yu, T., Wang, J., Lu, Y., Liu, W., Cheng, Y., 2017. Identification of long-range transport pathways and potential sources of $PM_{2.5}$ and PM_{10} in Beijing from 2014 to 2015. Journal of Environmental Sciences. 56, 214–229. https://doi.org/10.1016/j.jes.2016.06.035.

Li, J., Han, X., Jin, M., Zhang, X., Wang, S., 2019a. Globally analysing spatiotemporal trends of anthropogenic $PM_{2.5}$ concentration and population's $PM_{2.5}$ exposure from 1998 to 2016. Environment International. 128, 46–62. https://doi.org/10.1016/j.envint.2019.04.026.

Li, H., You, S., Zhang, H., Zheng, W., Lee, W-l., Ye, T., Zou, L., 2018. Analyzing the impact of heating emissions on air quality index based on principal component regression. Journal of Cleaner Production. 171: 1577–92. https://doi.org/10.1016/j.jclepro.2017.10.106.

Li, R., Li, Z., Gao, W., Ding, W., Xu, Q., Song, X., 2015. Diurnal, seasonal, and spatial variation of $PM_{2.5}$ in Beijing. Science Bulletin 60, 387–395. https://doi.org/10.1007/s11434-014-0607-9.

Li, Y., Shao, L., Wang, W., Zhang, M., Feng, X., Li, W., Zhang, D., 2019b. Airborne fiber particles: Types, size and concentration observed in Beijing. Science of The Total Environment 2019,705:135967. 10.1016/j.scitotenv.2019.135967.

Liang, X., Li, S., Zhang, S., Huang, H., Chen, S., 2016. $PM_{2.5}$ Data Reliability, Consistency and Air Quality Assessment in Five Chinese Cities. Journal of Geophysical Research: Atmospheres. 121(17): 10,220–10,36. https://doi.org/10.1002/2016JD024877.

Liu, Q., Liu, Y., Yin, J., Zhang, M., Zhang, T., 2014. Chemical characteristics and source apportionment of PM_{10} during Asian dust storm and non-dust storm days in Beijing. Atmospheric Environment. 91, 85–94. https://doi.org/10.1016/j.atmosenv.2014.03.057.

Liu, S., Xing, J., Wang, S., Ding, D., Chen, L., Hao, J., 2020. Revealing the impacts of transboundary pollution on $PM_{2.5}$-related deaths in China. Environment International. 134:105323. https://doi.org/10.1016/j.envint.2019.105323.

Liu, Z., Xie, M., Tian, K., Gao, P., 2017. GIS-based analysis of population exposure to $PM_{2.5}$ air pollution—A case study of Beijing. Journal of Environmental Sciences. 59: 48–53.

https://doi.org/10.1016/j.jes.2017.02.013.

Ma, Q., Wu, Y., Zhang, D., Wang, X., Xia, Y., Liu, X., Tian, P., Han, Z., Xia, X., Wang, Y., Zhang, R., 2017. Roles of regional transport and heterogeneous reactions in the $PM_{2.5}$ increase during winter haze episodes in Beijing. Science of The Total Environment. 599–600, 246–253. 10.1016/j.scitotenv.2017.04.193.

Maji, K.J., Ye, W.-F., Arora, M., Nagendra, S.M.S., 2019. Ozone pollution in Chinese cities: Assessment of seasonal variation, health effects and economic burden. Environmental Pollution. 247, 792–801. https://doi.org/10.1016/j.envpol.2019.01.049.

Meng, K., Xu, X., Cheng, X., Xu, X., Qu, X., Zhu, W., Ma, C., Yang, Y., Zhao, Y., 2018. Spatio-temporal variations in SO_2 and NO_2 emissions caused by heating over the Beijing-Tianjin-Hebei Region constrained by an adaptive nudging method with OMI data. Science of The Total Environment. 642, 543–552. https://doi.org/10.1016/j.scitotenv.2018.06.021.

MEP (Ministry of Ecology and Environment of the People's Republic of China), 2017. Action Plan for Comprehensive Control of Atmospheric Pollution in Autumn and Winter of Beijing-Tianjin-Hebei region in 2017–2018. http://www.mee.gov.cn/gkml/hbb/bwj/201708/t20170824_420330.htm (accessed 21 August 2017).

Nguyen, G.T.H., Shimadera, H., Uranishi, K., Matsuo, T., Kondo, A., 2019. Numerical assessment of $PM_{2.5}$ and O_3 air quality in Continental Southeast Asia: Impacts of potential future climate change. Atmospheric Environment. 2019, 215: 116901. https://doi.org/10.1016/j.atmosenv.2019.116901.

Qiu, X., Duan, L., Cai, S., Yu, Q., Wang, S., Chai, F., Gao, J., Li, Y., Xu, Z., 2017. Effect of current emission abatement strategies on air quality improvement in China: A case study of Baotou, a typical industrial city in Inner Mongolia. Journal of Environmental Sciences. 57: 383–90. http://dx.doi.org/10.1016/j.jes.2016.12.014.

Salim, I., Sajjad, R.U., Paule-Mercado, M.C., Memon, S.A., Lee, B-Y., Sukhbaatar, C., Lee, C-H., 2019. Comparison of two receptor models PCA-MLR and PMF for source identification and apportionment of pollution carried by runoff from catchment and sub-watershed areas with mixed land cover in South Korea. Science of The Total Environment. 663: 764–75. https://doi.org/10.1016/j.scitotenv.2019.01.377.

Sheehan, M.C., Lam, J., Navas-Acien, A., Chang, H.H., 2016. Ambient air pollution epidemiology systematic review and meta-analysis: A review of reporting and methods practice. Environment International. 92–93, 647–656. https://doi.org/10.1016/j.envint.2016.02.016.

Sun, C., Luo, Y., Li, J., 2018. Urban traffic infrastructure investment and air pollution: Evidence from the 83 cities in China. Journal of Cleaner Production. 172, 488–496. https://doi.org/10.1016/j.jclepro.2017.10.194.

Tan, K.C., San Lim, H., Jafri, M.Z.M., 2016. Prediction of column ozone concentrations using multiple regression analysis and principal component analysis techniques: A case study in peninsular Malaysia. Atmospheric Pollution Research. 7(3): 533–46. https://doi.org/10.1016/j.apr.2016.01.002.

Tao, W., Xue, L., Brimblecombe, P., Lam, Y., Li, L., Zhang, L., 2016. Ozone pollution in China: A review of concentrations, meteorological influences, chemical precursors, and effects. Science of The Total Environment. 575. https://doi.org/10.1016/j.scitotenv.2016.10.081.

The State Council of China, 2013. Air Pollution Prevention and Control Action Plan. http://www.gov.cn/zwgk/2013-09/12/content_2486773.htm (accessed 12 September 2013).

Tian, Y., Jiang, Y., Liu, Q., Xu, D., Zhao, S., He, L., Liu, H., Xu, H., 2019. Temporal and spatial trends in air quality in Beijing. Landscape and Urban Planning. 185, 35–43. https://doi.org/10.1016/j.landurbplan.2019.01.006.

UN Environment 2019. A Review of 20 Years' Air Pollution Control in Beijng. United Nations Environment Programme. Nairobi, Kenya.

Vu, T.V., Shi, Z., Cheng, J., Zhang, Q., He, K., Wang, S., Harrison, R.M., 2019. Assessing the impact of Clean Air Action Plan on Air Quality Trends in Beijing Megacity using a machine learning technique. Atmospheric Chemistry and Physics Discussions. 19(17): 11303–14. https://doi.org/10.5194/acp-19-11303-2019.

Wang, K., Yin, H., Chen, Y., 2019a. The effect of environmental regulation on air quality: A study of new ambient air quality standards in China. Journal of Cleaner Production. 215: 268–79. https://doi.org/10.1016/j.jclepro.2019.01.061.

Wang, N., Lyu, X., Deng, X., Huang, X., Jiang, F., Ding, A., 2019b. Aggravating O_3 pollution due to NOx emission control in eastern China. Science of The Total Environment. 677, 732–744. https://doi.org/10.1016/j.scitotenv.2019.04.388.

Wang, W., Chai, F., Zhang, K., Wang, S., Chen, Y., Wang, X., Yang, Y., 2008. Study on ambient air quality in Beijing for the summer 2008 Olympic Games. Air Quality Atmosphere & Health. 1(1): 31–36. 10.1007/s11869-008-0003-1.

Wang, W., Shao, L., Li, J., Chang, L., Zhang, D., Zhang, C., Jiang, J., 2019c. Characteristics of individual particles emitted from an experimental burning chamber with coal from the lung cancer area of Xuanwei, China. Aerosol and Air Quality Research. 19, 355–363. 10.4209/aaqr.2018.05.0187.

Wang, X., Shen, X., Sun, J., Zhang, X., Wang, Y., Zhang, Y., Wang, P., Xia, C., Qi, X., Zhong, J., 2018a. Size-resolved hygroscopic behavior of atmospheric aerosols during heavy aerosol pollution episodes in Beijing in December 2016. Atmospheric Environment. 194: 188–97. 10.1016/j.atmosenv.2018.09.041.

Wang, Y., Li, W., Gao, W., Liu, Z., Tian, S., Shen, R., Ji, D., Wang, S., Wang, L., Tao, S., Cheng, M., Wang, G., Gong, Z., Hao, J., Zhang, Y., 2019d. Trends in particulate matter and its chemical compositions in China from 2013–2017. Science China Earth Sciences. 10.1007/s11430-018-9373-1.

Wang, Y., Wang, Y., Tang, G., Song, T., Zhou, P., Liu, Z., Hu, B., Ji, D., Wang, L., Zhu, X., Yan, C., Ehn, M., Gao, W., Pan, Y., Xin, J., Sun, Y., Kerminen, V-M., Kulmala, M., and Petäjä, T., 2018b. Rapid formation of intense haze episode in Beijing. Atmospheric Chemistry & Physics Discussions. 1–18. https://doi.org/10.5194/acp-2018-1079.

Wang, Z., Li, Y., Chen, T., Zhang, D., Sun, F., Sun, R., Dong, X., Sun, N., Pan, L. (2014). Temporal and Spatial Distribution Characteristics of Ozone in Beijing. Environmental Science. 35(12): 4446–53. 10.13227/j.hjkx.2014.12.005.

Wang, Z., Zhang, D., Li, Y., Feng, P., Dong, X., Sun, R., Pan, L., 2015. Analysis of air quality in Beijing city during Spring Festival period of 2014. Acta Scientiae Circumstantiae. 35(2): 371–378. 10.13671/j.hjkxxb.2014.0798.

WHO report. Air pollution data of WHO. http://apps.who.int/gho/data/node.main.152?lang=en (accessed 16 May 2018).

Wu, J., Yao, F., Li, W., Si, M., 2016. VIIRS-based remote sensing estimation of ground-level $PM_{2.5}$ concentrations in Beijing–Tianjin–Hebei: A spatiotemporal statistical model. Remote Sensing of Environment. 184, 316–328. https://doi.org/10.1016/j.rse.2016.07.015.

Xiang, S., Liu, J., Tao, W., Yi, K., Xu, J., Hu, X., Liu, H., Wang, Y., Zhang, Y., Yang, H., Hu, J., Wan, Y., Wang, X., Ma, J., Wang, X., Tao, S., 2020. Control of both $PM_{2.5}$ and O_3 in Beijing-Tianjin-Hebei and the surrounding areas. Atmospheric Environment. 224: 117259. https://doi.org/10.1016/j.atmosenv.2020.117259.

Xu, S., Ge, J., 2020. Sustainable shifting from coal to gas in North China: An analysis of resident satisfaction .Energy Policy. 138: 111296. https://doi.org/10.1016/j.enpol.2020.111296.

Xu, X., Jiang, Z., Li, J., Chu, Y., Tan, W., Li, C., 2020. Impacts of meteorology and emission control on the abnormally low particulate matter concentration observed during the winter of 2017. Atmospheric Environment. 225: 117377. https://doi.org/10.1016/j.atmosenv.2020.117377.

Xu, X., Zhang, T., 2020. Spatial-temporal variability of $PM_{2.5}$ air quality in Beijing, China during 2013–2018. Journal of Environmental Management. 262: 110263. https://doi.org/10.1016/j.jenvman.2020.110263.

Xue, T., Liu, J., Zhang, Q., Geng, G., Zheng, Y., Tong, D., Liu, Z., Guan, D., Bo, Y., Zhu, T., He, K., Hao, J., 2019. Rapid improvement of $PM_{2.5}$ pollution and associated health benefits in China during 2013–2017. Science China(Earth Sciences). 62(12): 1847–56. https://doi.org/10.1007/s11430-018-9348-2.

Yang, X., Liu, S., Shao, P., He, J., Liang, Y., Zhang, B., Liu, B., Liu, Y., Tang, G., Ji, D., 2020. Effectively controlling hazardous airborne elements: Insights from continuous hourly observations during the seasons with the most unfavorable meteorological conditions after the implementation of the APPCAP. Journal of Hazardous Materials. 387: 121710. https://doi.org/10.1016/j.jhazmat.2019.121710.

Zhan, D., Kwan, M-P., Zhang, W., Yu, X., Meng, B., Liu, Q., 2018. The driving factors of air quality index in China. Journal of Cleaner Production. 197: 1342–51. 10.1016/j.jclepro.2018.06.108.

Zhang, H., Cheng, S., Li, J., Yao, S., Wang, X., 2019a. Investigating the aerosol mass and chemical components characteristics and feedback effects on the meteorological factors in the Beijing-Tianjin-Hebei region, China. Environmental Pollution. 244, 495–502. https://doi.org/10.1016/j.envpol.2018.10.087.

Zhang, H., Wang, S., Hao, J., Wang, X., Wang, S., Chai, F., Li, M., 2016. Air pollution and control action in Beijing. Journal of Cleaner Production. 112, 1519–1527. https://doi.org/10.1016/j.jclepro.2015.04.092.

Zhang, M., Shan, C., Wang, W., Pang, J., Guo, S., 2020. Do driving restrictions improve air quality: Take Beijing-Tianjin for example? Science of The Total Environment. 712: 136408. https://doi.org/10.1016/j.scitotenv.2019.136408.

Zhang, Q., Ma, Q., Zhao, B., Liu, X., Wang, Y., Jia, B., Zhang, X., 2018. Winter haze over North China Plain from 2009 to 2016: Influence of emission and meteorology. Environmental Pollution. 242:1308–18. 10.1016/j.envpol.2018.08.019.

Zhang, Q., Zheng, Y., Tong, D., Shao, M., Wang, S., Zhang, Y., Xu, X., Wang, J., He, H., Liu, W., Ding, Y., Lei, Y., Li, J., Wang, Z., Zhang, X., Wang, Y., Cheng, J., Liu, Y., Shi, Q., Yan, L., Geng, G., Hong, C., Li, M., Liu, F., Zheng, B., Cao, J., Ding, A., Gao, J., Fu, Q., Huo, J., Liu, B., Liu, Z., Yang, F., He, K., 2019b. Drivers of improved $PM_{2.5}$ air quality in China from 2013 to 2017. Proceedings of the National Academy of Sciences. 116:201907956. 10.1073/pnas.1907956116.

Zhang, S., Guo, B., Dong, A., He, J., Xu, Z., Chen, S., 2017. Cautionary tales on air-quality improvement in Beijing. Proceedings of the Royal Society A: Mathematical, Physical and Engineering Science. 473, 20170457. 10.1098/rspa.2017.0457.

Zhang, X., Xu, X., Ding, Y., Liu, Y., Zhang, H., Wang, Y., Zhong, J., 2019c. The impact of meteorological changes from 2013 to 2017 on $PM_{2.5}$ mass reduction in key regions in China. Science China Earth Sciences. 62. https://doi.org/10.1007/s11430-019-9343-3.

Zhang, Y. L., 2019. Dynamic effect analysis of meteorological conditions on air pollution: A case study from Beijing. Science of The Total Environment. 684: 178–85. https://doi.org/10.1016/j.scitotenv.2019.05.360.

Zheng, G., Duan, F., Su, H., Ma, Y., Cheng, Y., Zheng, B., Zhang, Q., Huang, T., Kimoto, T., Chang, D., Pöschl, U., Cheng, Y., He, K., 2015. Exploring the severe winter haze in Beijing: The impact of synoptic weather, regional transport and heterogeneous reactions. Atmospheric Chemistry and Physics. 15, 2969–2983. 10.5194/acp-15-2969-2015.

Figures

Figure 1 The distribution map of automatic air quality ground monitoring stations in Beijing.

Figure 2 The distributions of days under different air quality levels and the annual mean of AQI in Beijing.

Figure 3 Time-series of the daily average of AQI in Beijing.

Figure 4 Time-series of the daily, monthly, and seasonal concentrations of (a) $PM_{2.5}$, (b) PM_{10}, (c) SO_2, (d) CO, (e) NO_2, (f) O_3 between January 2013 and February 2020 in Beijing.

Figure 5 The concentration of $PM_{2.5}$, PM_{10}, SO_2, NO_2, CO, and O_3 in the heating period and the non-heating period at stage I and stage II in Beijing.

Figure 6 Spatial distributions of $PM_{2.5}$, PM_{10}, SO_2, NO_2, CO, and O_3 in the heating period and the non-heating period at stage I and stage II in Beijing.

Figure 7 Comparison of observed (black line) and simulated (red line) monthly average of (1) $PM_{2.5}$, (2) PM_{10}, (3) SO_2, (4) NO_2, (5) CO, and (6) O_3 in Beijing.

Figure 8 Comparison of the stimulated monthly average concentration of PM2.5 by PCA-MNLR and WRF-CMAQ (Cheng et al., 2019x).

Figure 9 The score plot of PC1 and PC2 by the PCA method.

Figure 10 The variations of air pollutant emission during 2010–2018 in Beijing.

Figure 11 The variations of (a) energy consumption structure, and (b) socio-economic in Beijing, 2010–2018.

Figure 12 The comparison of the annual mean concentration of $PM_{2.5}$ in different capital cities worldwide in 2013 and 2018.

Tables

Table 1 Sub-index of air pollutants and the corresponding concentration limits of different AQI levels.

Table 2 The different levels of AQI values and the corresponding health implications and cautionary statement.

Table 3 Air quality standards for air pollutants set by the Chinese government and other countries. Table 4 The major control measures of the Clean Air Action and the Comprehensive Action.

Table 5 Annual mean concentration of air pollutants in Beijing.

Table 6 A comparison of the annual mean concentrations of air pollutants after the meteorological normalization from this study and other references.

Note: Some explanations and descriptions of the above figures and tables were added after their titles. Please see the detailed text below.

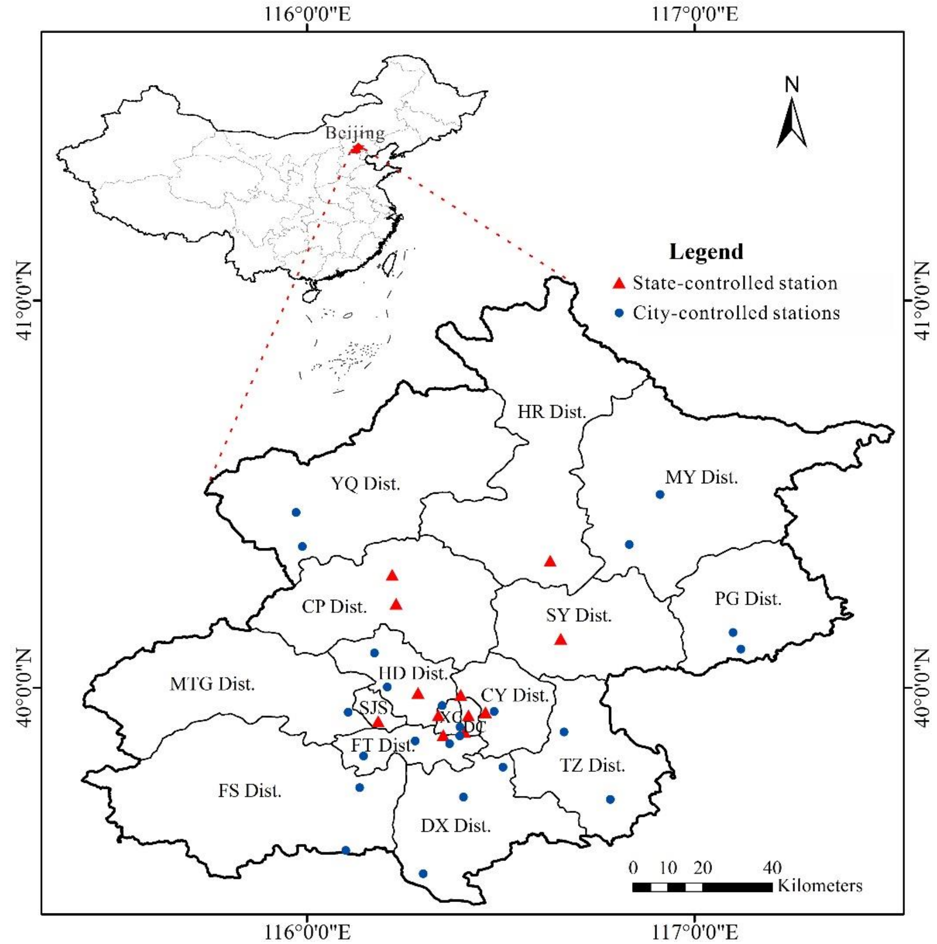

Fig. 1. The distribution map of automatic air quality ground monitoring stations in Beijing.

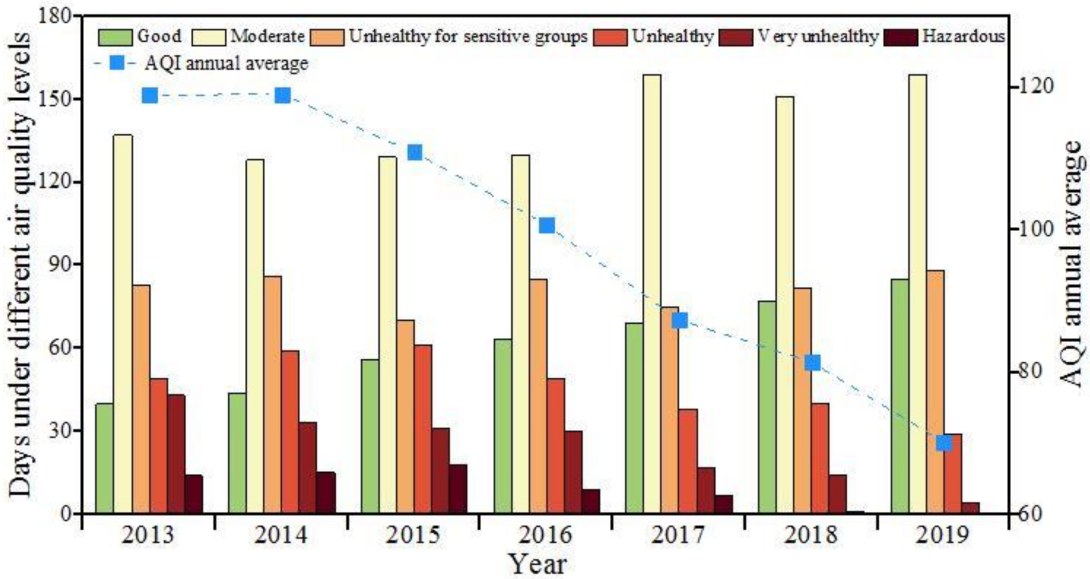

Fig. 2. The distributions of days under different air quality levels and the annual mean of AQI in Beijing. Meet-standard days include good air quality days and moderate air quality days, and heavy pollution days include very unhealthy days and hazardous days. Note: the annual mean of AQI decreased yearly, good air quality days increased most, and hazardous days decreased most.

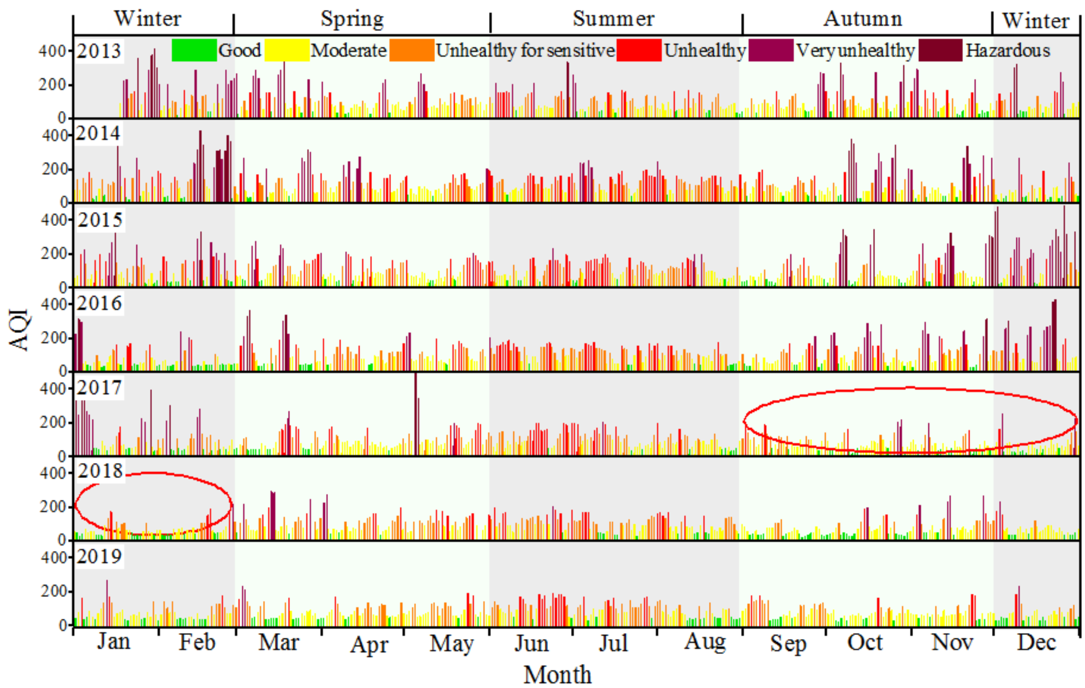

Fig. 3. Time-series of the daily average of AQI in Beijing. Please note that the red circled areas refer to autumn and winter in 2017 where the daily values of AQI had a significant decrease.

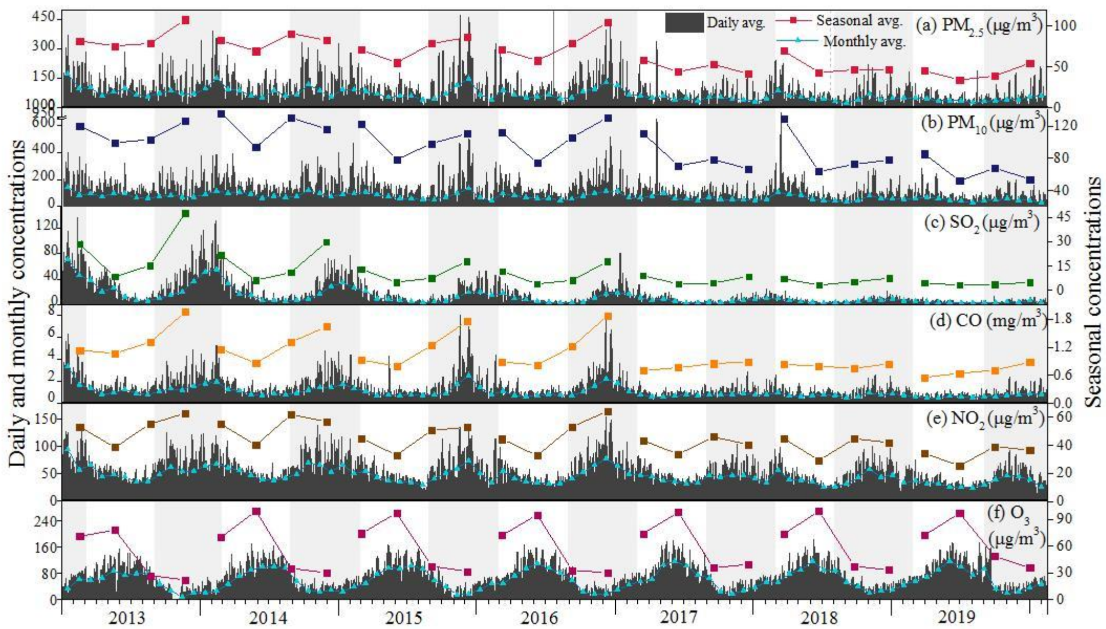

Fig. 4. Time-series of the daily, monthly, and seasonal concentrations of (a) $PM_{2.5}$, (b) PM_{10}, (c) SO_2, (d) CO, (e) NO_2, (f) O_3 between January 2013 and February 2020 in Beijing. Grey colors in the background refer to autumn (September to November) and winter (December to February), and light colors refer to spring (March to May) and summer (June to August). Note: SO_2 and CO decreased obviously and tended to be flat, and $PM_{2.5}$, PM_{10}, and NO_2 decreased but still fluctuated, while O_3 increased with a different seasonal distribution compared to other pollutants.

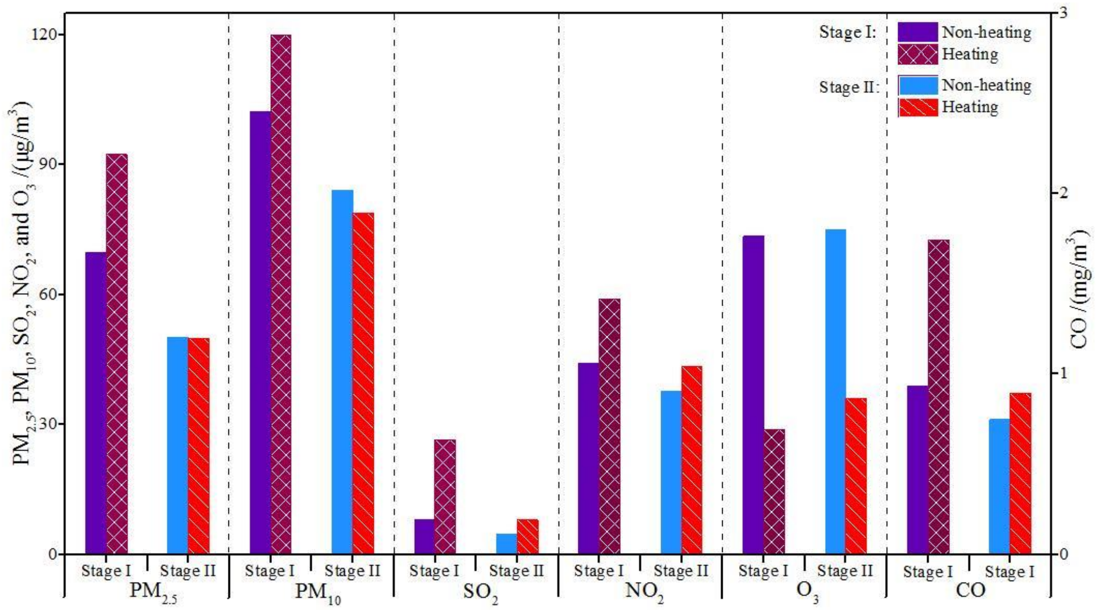

Fig. 5. The concentration of $PM_{2.5}$, PM_{10}, SO_2, NO_2, CO, and O_3 in the heating period and the non-heating period at stage I and stage II in Beijing. The heating period is from November 15 to March 15, and the non-heating period is from March 16 to November 14. Note: At stage I, the air pollutant concentration was higher in the heating period, but at stage II these decreased dramatically, $PM_{2.5}$ and PM_{10} were lower in the heating period. However, O_3 was increased in both the heating and non-heating period.

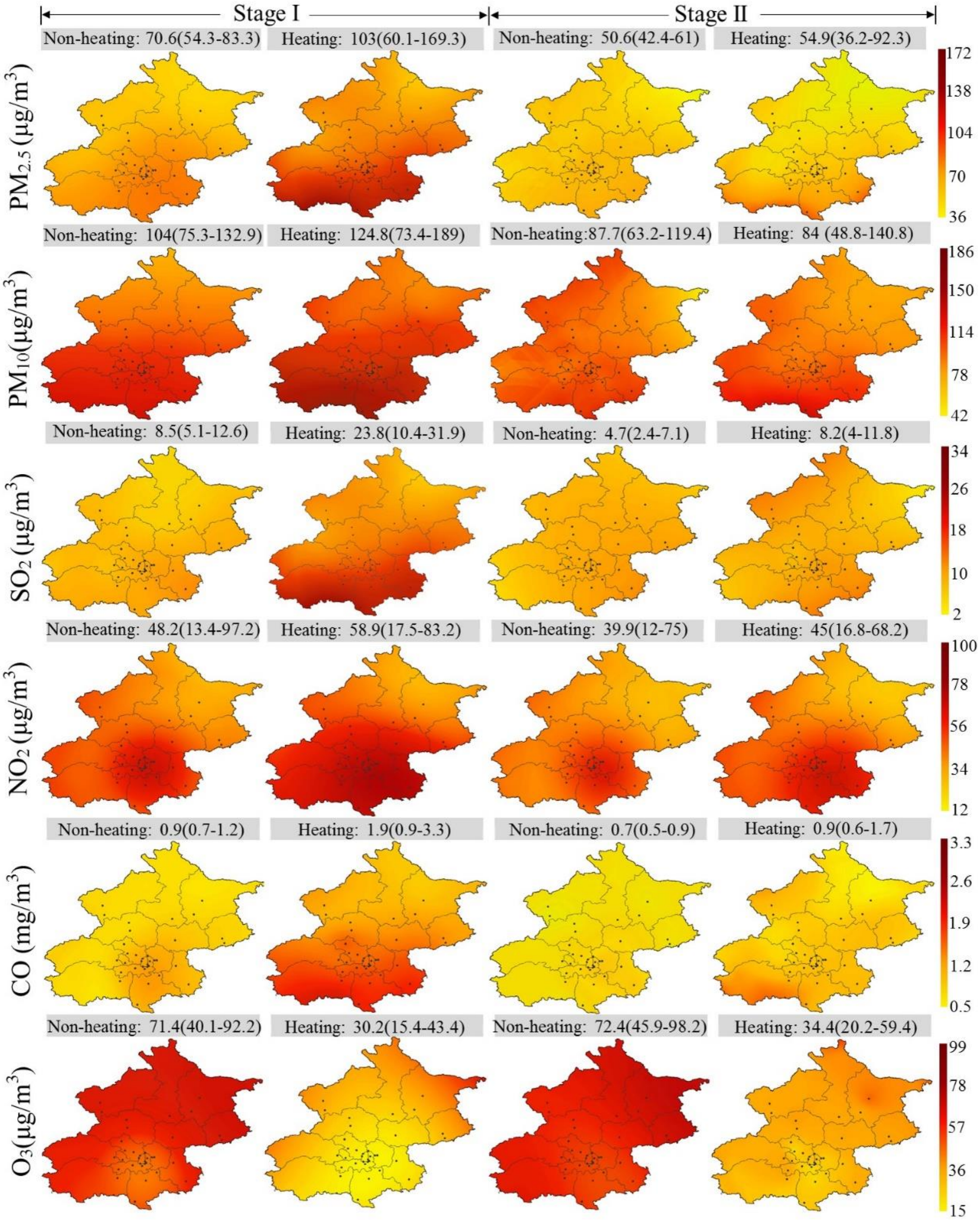

Fig. 6. Spatial distributions of $PM_{2.5}$, PM_{10}, SO_2, NO_2, CO, and O_3 in the heating period and the non-heating period at stage I and stage II in Beijing. The numbers above each picture signify the average value (outside) and variation range (inside the bracket). Note: air pollutants decreased significantly in the heating period at stage II. O_3 had a different changing pattern and increased at stage II. The southern region had a more serious pollution situation.

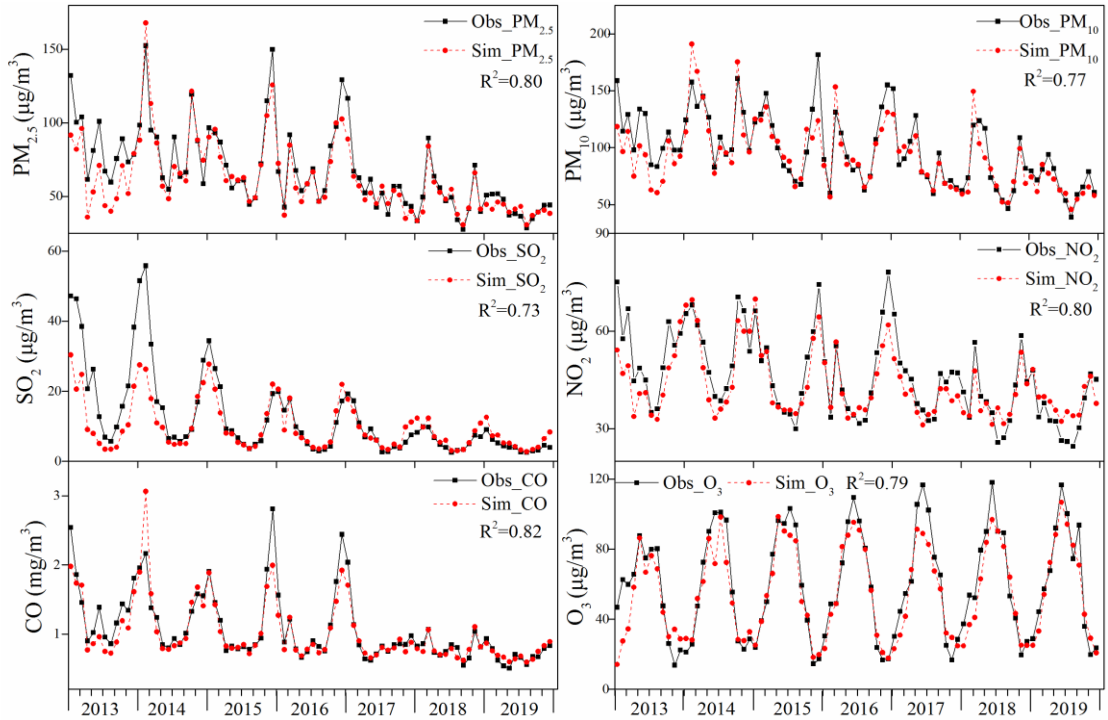

Fig. 7. Comparison of observed (black line) and simulated (red line) monthly average of (1) $PM_{2.5}$, (2) PM_{10}, (3) SO_2, (4) NO_2, (5) CO, and (6) O_3 in Beijing. Note: the meteorological normalized values of major air pollutants were lower during 2013–2016, but these values became higher than the observed values after 2017, which indicated the more beneficial weather conditions in 2017.

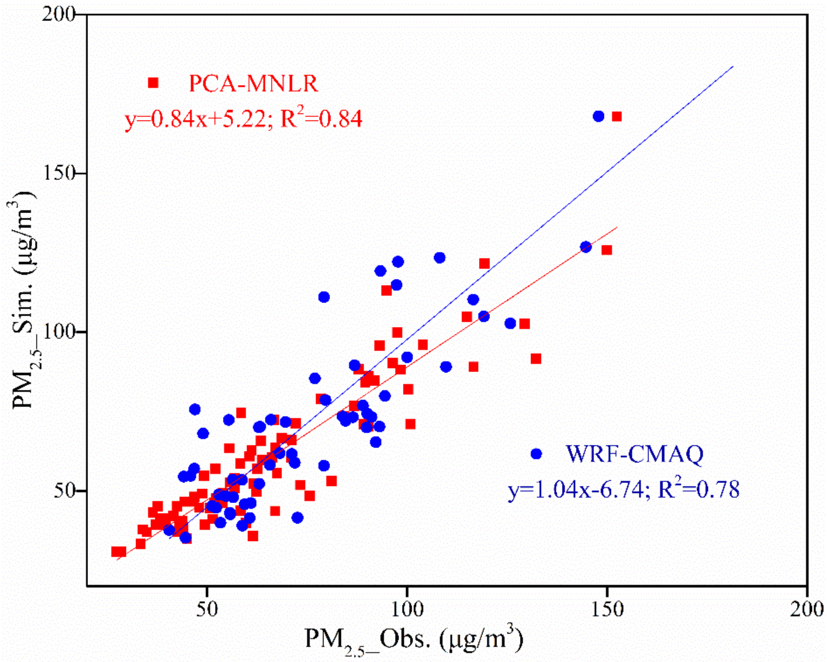

Fig. 8. Comparison of the stimulated monthly average concentration of $PM_{2.5}$ by PCA-MNLR (this study) and WRF-CMAQ (Cheng et al., 2019a).

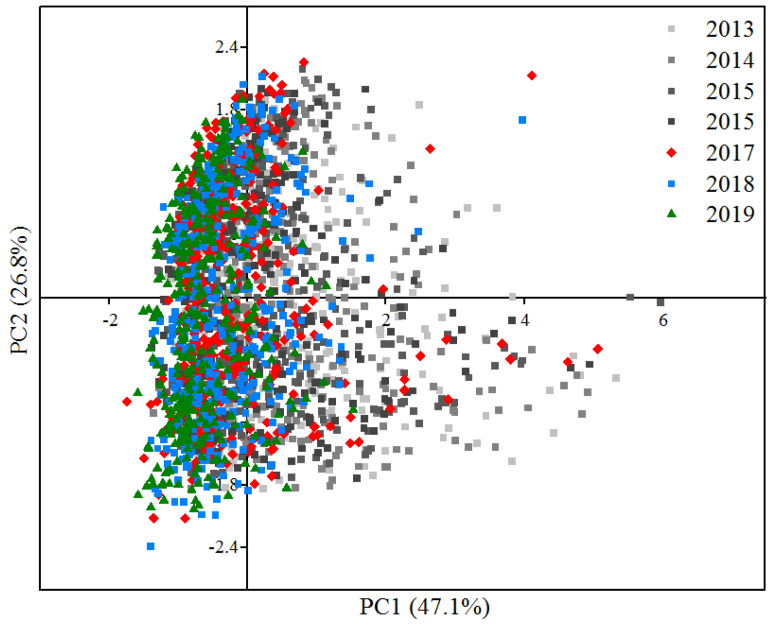

Fig. 9. The score plot of PC1 and PC2 by the PCA method. Note: The PCs dots had descending x-axis values, indicating the significant decrease of heavy pollution days after 2017.

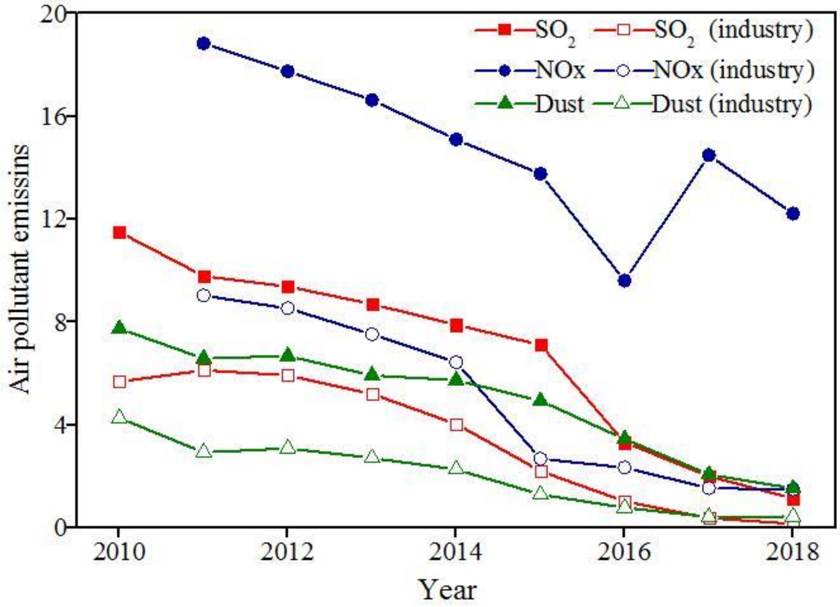

Fig. 10. The variations of air pollutant emission during 2010–2018 in Beijing. Data came from the Beijing Statistical Yearbooks (BSY, 2019). Unit: 10,000 tons. Note: SO_2 and dust emissions decreased gradually, while NOx emission had a fluctuant decrease.

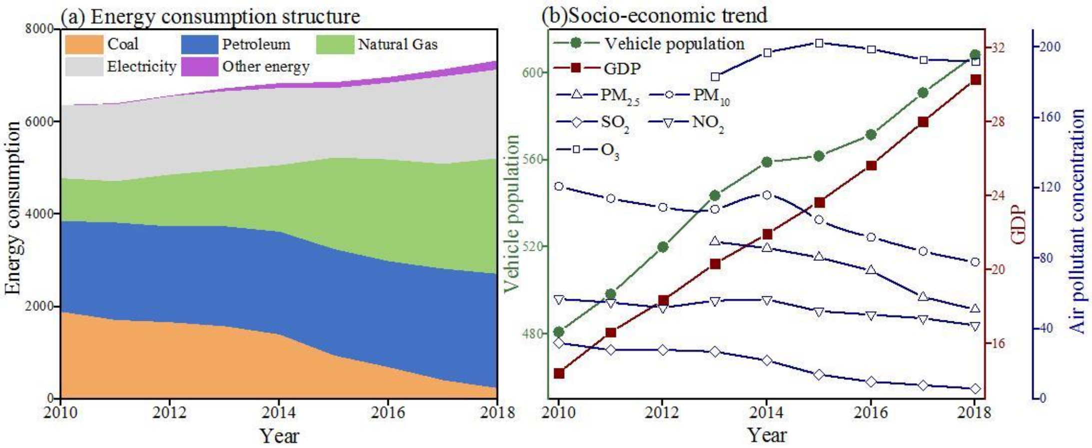

Fig. 11. The variations of (a) energy consumption structure, and (b) socio-economic in Beijing, 2010–2018. Data came from the Beijing Statistical Yearbooks (BSY, 2019). Unit: 10,000 tons of SCE for (a) energy consumption structure; 10,000 units for vehicle population, 100 billion yuan for GDP, μg/m^3 for $PM_{2.5}$, PM_{10}, SO_2, NO_2, and O_3. Note: Coal consumption decreased significantly, with steady socio-economic growth and gradual air pollutants decrease.

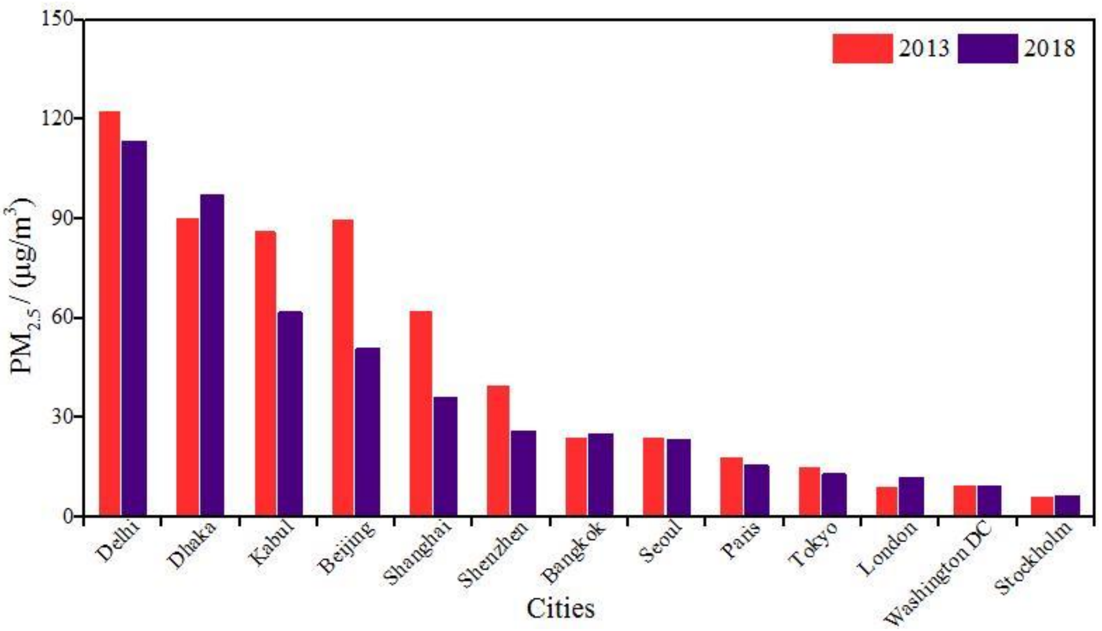

Fig. 12. The comparison of the annual mean concentration of $PM_{2.5}$ in different capital cities worldwide in 2013 and 2018. Data came from a World Health Organization report (WHO Report). Note: $PM_{2.5}$ of Beijing is still higher than some capital cities of developed countries, some Asian cities, and some domestic cities, and also is lower than some cities of developing countries.

Table 1

Sub-index of air pollutants and the corresponding concentration limits of different AQI levels. Unit: μg/m^3 for all air pollutants, except CO (mg/m^3).

IAQI	$PM_{2.5}$	PM_{10}	SO_2		NO_2		O_3		CO	
	24h[1]	24h[1]	24h[1]	1h[2]	24h[1]	1h	8h[3]	1h	24h[1]	1h
0	0	0	0	0	0	0	0	0	0	0
50	35	50	50	150	40	100	100	160	2	5
100	75	150	150	500	80	200	160	200	4	10
150	115	250	475	650	180	700	215	300	14	35
200	150	350	800	800	280	1200	265	400	24	60
300	250	420	1600	-	565	2340	800	800	36	90
400	350	500	2100	-	750	3090	-	1000	48	120
500	500	600	2620	-	940	3840	-	1200	60	150

[1] the daily average of $PM_{2.5}$, PM_{10}, SO_2, NO_2, and CO is used in daily evaluation;

[2] the hourly average of SO_2, NO_2, O_3, and CO is only used in the hourly evaluation. When the hourly average of SO_2 exceeds 800 μg/m^3, the hourly IAQI will not be calculated and the daily concentration should be used instead.

[3] when the 8 hour average of O_3 exceeds 800, the 8-hour IAQI will not be calculated and the hourly concentration should be used instead.

Table 2

The different levels of AQI values and the corresponding health implications and cautionary statement.

AQI values	AQI levels	Air quality level	Health implications	Cautionary statement
0–50	I	Good	Air quality is considered satisfactory, and air pollution poses little or no risk.	Everyone can do normal activities.
51–100	II	Moderate	Air quality is acceptable; however, some pollutants may have a moderate health concern for a very small number of people with abnormal sensitivity.	A very small number of people with abnormal sensitivity should limit outdoor exertion.
101–150	III	Unhealthy for sensitive groups	Members of sensitive groups may have a mild increase in symptoms. The general public may experience irritation symptoms.	Children, the elderly, and people with heart and respiratory disease should limit prolonged and intense outdoor exertion.
151–200	IV	Unhealthy	Members of sensitive groups may have further aggravated symptoms. The general public may experience an impact on the heart and respiratory symptoms.	Children, the elderly, and people with heart and respiratory disease should limit prolonged and intense outdoor exertion; everyone else should properly limit outdoor exertion.
201–300	V	Very unhealthy	Patients with heart and lung disease may have significantly increased symptoms and decreased exercise tolerance. The general public may widely experience symptoms.	Children, the elderly, and people with heart and lung disease, should stay indoors and stop outdoor exertion; everyone else should limit outdoor exertion.
>300	VI	Hazardous	The general public may have decreased exercise tolerance and obvious strong symptoms and may have some diseases in advance.	Children, the elderly, and patients should stay indoors and avoid physical exertion; everyone else should avoid outdoor exertion.

Table 3

Air quality standards for air pollutants set by the Chinese government and other countries.

Pollutant	Time	China I[1]	China II[1]	WHO 2006	USA I	USA II	European Union	Japan	South Korea	India	Australia
$PM_{2.5}$ ($\mu g/m^3$)	yearly	15	35	10	12	15	25	15	25	40	8
	daily	35	75	25	35	35		35	50	60	25
PM_{10} ($\mu g/m^3$)	yearly	40	70	20	-	-	40	-	50	60	-
	daily	50	150	50	150	150	50	80	100	100	50
SO_2 ($\mu g/m^3$)	yearly	20	60		-	-		-	0.02[2]	50	0.02[2]
	daily	50	150	20	-	-	125	0.04[2]	0.05[2]	80	0.08[2]
	hourly	150	500	-	75[2]	0.05[3,4]	300	0.1[2]	0.15[2]	-	0.2[2]
NO_2 ($\mu g/m^3$)	yearly	40	40	40	53[3]	53[3]	40	-	0.03[2]	40	0.03[2]
	daily	80	80		-	-		0.04	0.06[2]	80	-
	hourly	200	200	200	100[3]	-	200	-	0.1[2]	-	0.12[2]
CO (mg/m^3)	1 day	4	4	-	-	-	-	10[2]	-	-	-
	8 hours			10	9[2]	-	10	20[2]	9[2]	2	9[2]
	hourly	10	10	30	35[2]	-	-	-	25[2]	4	-
O_3 ($\mu g/m^3$)	8 hours	100	160	100	0.07[2]	0.07[2]	120	-	0.06[2]	100	-
	4 hours			-	-	-	-	-	-	-	0.08[2]
	1 hour	160	200		-	-		60	0.1[2]	180	0.1[2]

[1] China I is the first-level concentration limit of China national ambient air quality standards (NAAQS-I), suitable for the ecologically sensitive areas, tourist attractions, and other areas required special protection. China II is the second-level concentration limit of China national ambient air quality standards (NAAQS-II), suitable for industrial, residential, rural, and other areas.

[2] units refer to parts per million (ppm).

[3] units refer to parts per billion (ppb).

[4] the average value of 3 hours.

data source: China (http://www.mee.gov.cn/). USA (https://www.epa.gov/criteria-air-pollutants).

Table 4

The major control measures of the Clean Air Action and the Comprehensive Action. A refer to the Clean Air Action, and B refers to the Comprehensive Action. This classification of pollution sources is depended on the classification in the source apportionment from Beijing Ecology and Environmental Statement 2018.

Action	Pollution source	Measures
A	Coal-fired emissions	(1) Adjust and optimize the energy structure. (2) Utilize clean coal. (3) Increase clean energy alternatives such as coal-to-gas or coal-to-electricity, and increase clean energy sources such as hydropower, wind power, and solar energy. (4) Renovate or eliminate coal-fired boilers. (5) Improve energy efficiency. (6) Eliminate civil bulk coal consumption.
	Industrial emissions	(1) Adjust industrial structure, optimize the industrial layout, and promote industrial upgrade. (2) Rectify polluting businesses and enterprises. (3) Eliminate or upgrade industries with excessive, backward, and polluting industries. (4) Reduce volatile organic compounds (VOCs) emission. (5) Promote cleaner production (CP). (6) Accelerate the technological transformation and improve innovation capability.
	Vehicle emissions	(1) Make strict standards for new vehicles. (2) Retrofit in-use vehicles, eliminate "yellow-labeled" vehicles, and retire old vehicles. (3) Improve fuel quality and develop new energy vehicles. (4) Optimize traffic structure.
	Dust emissions	(1) Increase the quality and frequency of the road cleaning process. (2) Shut down concrete mixing plants and update cinder block transporters. (3) Make an afforestation project.
	Other measures	(1) Improve environmental law, regulation system, and economic policy. (2) Enhance atmospheric environmental supervision capability. (3) Establish regional coordination mechanisms. (4) Monitor emergency response systems to deal with heavy pollution events. (5) Mobilize public participation.
B	Coal-fired emission	(1) Partial halt production in the steel industry. (2) Full halt production in the building material industries, and optimization of production control in the nonferrous chemical industries. (3) Full halted production in the cement powder stations during the heavy pollution emergency period.
	Others	Other measures carried out are according to the “Clean Air Action”.

Table 5

The annual mean concentration of air pollutants in Beijing. Data came from Beijing's ecology and environment statement.

Year	$PM_{2.5}$ (μg/m^3)	PM_{10} (μg/m^3)	SO_2 (μg/m^3)	CO-24h (mg/m^3)	NO_2 (μg/m^3)	O_3-8h (μg/m^3)
2013	89.5	108.1	26.5	3.4	56.0	183.4
2014	85.9	115.8	21.8	3.2	56.7	197.2
2015	80.6	101.5	13.5	3.6	50.0	202.6
2016	72.6	92.0	10.0	3.2	48.0	199.0
2017	58.0	84.0	8.0	2.1	46.0	193.0
2018	51.0	78.0	6.0	1.7	42.0	192.0
2019	42.0	68.0	4.0	1.4	37.0	191.0
NAAQS II	35.0	70.0	60.0	4.0	40.0	160.0

Supplement of

Air quality improvement in response to intensified control strategies in Beijing during 2013–2019

CONTENTS

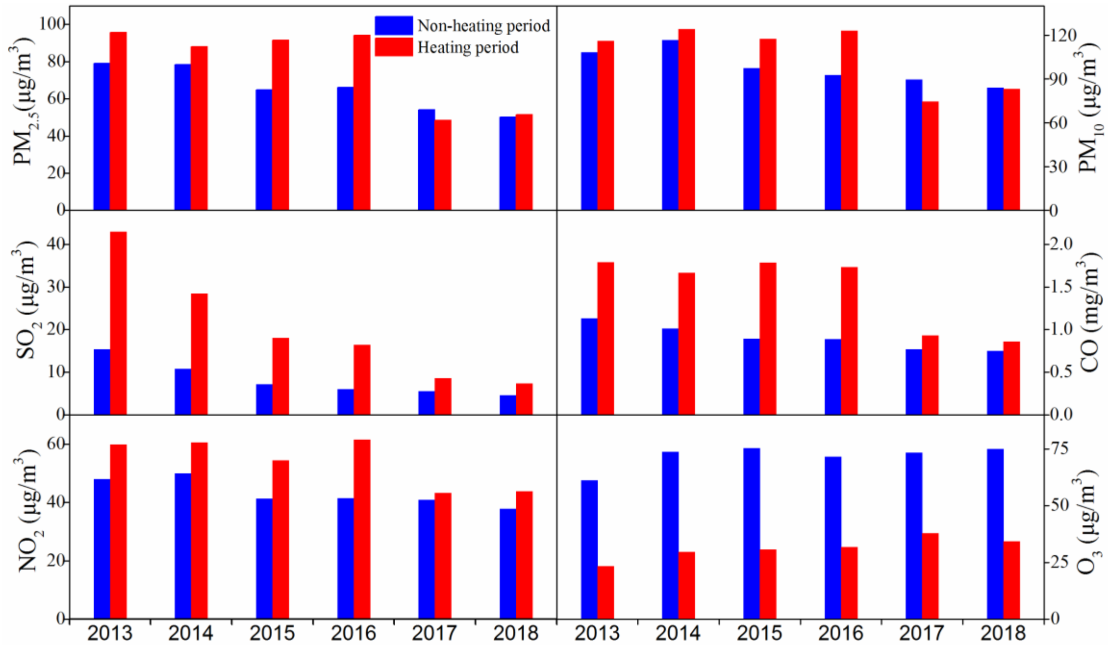

Fig. S1. The concentration of (a) $PM_{2.5}$, (b) PM_{10}, (c)SO_2, (d) CO, (e) NO_2, (f) O_3 in the heating period and the non-heating period during 2013–2019 in Beijing. Note: The concentrations of pollutants in the heating period decreased yearly, especially after 2017, except O_3. The data of this study included January 2013 to February 2020, which didn't cover the heating period of 2019. For that reason, the heating period and the non-heating period of 2019 were not compare in this figure.

Table S1

The measurement method and instrument of each pollutant. Note: Calibrations were strictly adhered according to Technical specifications for operation and quality control of ambient air quality continuous automated monitoring system for SO_2, NO_2, O_3, and CO (HJ 808-2018) and particulate matter (HJ 817-2018).

Pollutants	Method	Instrument
$PM_{2.5}$	Tapered element oscillating microbalance (TEOM)	Thermo Fisher 1405F
PM_{10}	Tapered element oscillating microbalance (TEOM)	Thermo Fisher 1400
SO_2	Ultraviolet fluorescence method	Thermo Fisher 43i
NO/NO_2/ NOx	Chemiluminescence (CL) method	Thermo Fisher 42C
CO	Gas filter infrared absorption method	Thermo Fisher 48C
O_3	Ultraviolet spectrophotometry method	Thermo Fisher 49C

Table S2

A comparison of the annual mean concentrations of air pollutants after the meteorological normalization from this study and other references.

Pollutant	Year	Obs.	Sim.	Others	Pollutant	Year	Obs.	Sim.	Others
$PM_{2.5}$ (μg/m^3)	2013	89.5	80.6	93[1], 86[2]	NO_2 (μg/m^3)	2013	56.0	54.8	58[1], 63[2]
	2014	85.9	86.8	85[1], 83[2]		2014	56.7	53.2	56[1], 61[2]
	2015	80.6	75.7	75[1], 75[2]		2015	50.0	48.6	50[1], 57[2]
	2016	73.0	68.1	71[1], 70[2]		2016	48.0	46.2	48[1], 56[2]
	2017	58.0	53.1	61[1], 54[2]		2017	46.0	42.7	48[1], 55[2]
	2018	51.0	49.2	-		2018	42.0	39.7	-
	2019	42.0	40.5	-		2019	37.0	36.3	-
PM_{10} (μg/m^3)	2013	108.1	113.5	123[1], 124[2]	CO* (mg/m^3)	2013	1.4	1.2	1.5[1], 1.2[2]
	2014	115.8	122.7	121[1], 128[2]		2014	1.3	1.4	1.3[1], 1.2[2]
	2015	101.5	105.5	106[1], 106[2]		2015	1.3	1.2	1.2[1], 1.1[2]
	2016	92.0	95.5	101[1], 103[2]		2016	1.1	1.0	1.1[1], 1.1[2]
	2017	84.0	86.2	93[1], 96[2]		2017	0.9	0.9	1.0[1], 1.1[2]
	2018	78.0	79.5	-		2018	0.8	0.8	-
	2019	68.0	64.8	-		2019	0.7	0.7	-
SO_2 (μg/m^3)	2013	26.5	20.4	26.3[1], 37[2]	O_3* (μg/m^3)	2013	55.6	47.3	59[1], 47[2]
	2014	21.8	18.6	20[1], 28[2]		2014	57.4	53.0	56[1], 46[2]
	2015	13.5	11.6	13[1], 19[2]		2015	59.0	56.2	59[1], 44[2]
	2016	10.0	10.1	10[1], 15[2]		2016	58.1	56.3	60[1], 49[2]
	2017	8.0	8.8	8.4[1], 11[2]		2017	60.4	53.1	61[1], 49[2]
	2018	6.0	7.2	-		2018	62.5	56.2	-
	2019	4.0	5.8	-		2019	62.8	59.9	-

[1] data is from Vu et al. (2019);

[2] data is from Cheng et al. (2019a);

* the annual mean concentration of CO and O_3 is calculated by daily average concentration, which is different from the official data.